

Technical Report

WIND WAVES AND THE REAERATION COEFFICIENT
IN OPEN CHANNEL FLOW

by

Aziz F. Eloubaidy

Erich J. Plate

Johannes Gessler

Prepared under

National Science Foundation

Grant No. GK 2142

Fluid Dynamics and Diffusion Laboratory
Civil Engineering Department
Colorado State University
Fort Collins, Colorado
August 1969

CER69-70AFE2



U18401 0575332

ABSTRACT

WIND WAVES AND THE REAERATION COEFFICIENT IN OPEN CHANNEL FLOW

The reaeration rates with and without wind blowing along the water surface have been studied in the laboratory.

The reaeration results, without wind, have been compared with those obtained by previous investigators.

Based on the concept that the reaeration rate is controlled by an effective turbulent diffusion coefficient at the surface and by rate of surface renewal, an equation was developed to predict reaeration rates in natural streams and rivers with wind blowing over the water surface. The state of turbulence, beneath the water surface, was considered as a good measure of the rate of surface renewal. The experimental results gave support to the theoretically developed equation.

The properties of water surface give good agreement with the results reported by previous investigators.

Experimental results indicate that reaeration rates are significantly increased when waves appear on the surface. The increase is very much more than can be accounted for by the increase in surface area. The increase was attributed to the dynamic effect of separation, occurring at the lee side of the waves.

Aziz F. Eloubaidy
Fluid Mechanics Program
Civil Engineering Department
Fort Collins, Colorado 80521
August 1960

ACKNOWLEDGMENTS

Acknowledgment is made to Dr. J.D. Vaughn, Dr. J.C. Ward, Dr. J. Gessler, and Dr. E.J. Plate for their contributions to the completion of this study, and the financial assistance afforded by the National Science Foundation.

A particular expression of appreciation is extended to Dr. Plate, the author's major professor, for his able direction and guidance throughout the experimental study and writing of this dissertation, and to Dr. Gessler, for his stimulating and constructive discussions during the final revisions of this work.

The scholarship given to the author by the Iraqi Government is gratefully acknowledged.

Special thanks is extended to Peter Liu for his help in the data collection and to Carlos Oporto for his assistance in reducing the data.

To his wife and family, whose sacrifices have made it possible for him to complete his studies, goes the author's deep gratitude.

TABLE OF CONTENTS

<u>Chapter</u>	<u>Page</u>
LIST OF TABLES	ix
LIST OF FIGURES.	x
LIST OF SYMBOLS.xii
I INTRODUCTION	1
Stream Reaeration	1
Wind-Waves and Reaeration	1
Research Objectives	3
Research Procedure.	4
II REVIEW OF LITERATURE	5
Theories of Gas Absorption Mechanism.	5
Basic equations of molecular diffusion.	5
The oxygen sag equation	7
The two film theory	9
The penetration theory.	11
Danckwerts' modified penetration theory.	12
The Kishinevski theory.	13
The Effect of Temperature on Reaeration	16
Previous Work on Stream Reaeration.	17
Summary on stream reaeration.	28
Prediction of Longitudinal Dispersion Coefficient	29
Dispersion in open channel flow	29
The Wind-Water Surface Interaction: Consequences.	33

TABLE OF CONTENTS - Continued

<u>Chapter</u>		<u>Page</u>
	Consequences: Turbulence.	33
	Estimation of water surface shear stress	34
III	THEORETICAL ANALYSIS.	37
	Development of the Formula	37
	Estimation of the vertical turbulent diffusion coefficient, averaged over depth.	38
	Estimation of the turbulent dif- fusion coefficient at the interface.	43
	The prediction equation for reaeration with wind	45
IV	EQUIPMENT AND PROCEDURES.	47
	The Wind Tunnel Flume Combination.	47
	The flume.	47
	Bed roughness.	50
	Air Flow	50
	Measurements of Water Surface Elevations	53
	Measurements of Dissolved Oxygen Concentrations	55
	The sensor	55
	Calibration of the Beckman's oxygen analyzer.	56
	Measuring Devices.	62
	Measurement of the Reaeration Coefficient.	62
	Experimental procedure	63
	Data Collections	64

TABLE OF CONTENTS - Continued

<u>Chapter</u>	<u>Page</u>
Reaeration with no air blowing. . . .	64
Reaeration with the air blowing	65
V DATA REDUCTION TECHNIQUES.	68
Summary of Experiments.	68
Determination of the Reaeration Coefficient for a Given Section	70
Estimation of the Longitudinal Dispersion Coefficient.	72
Longitudinal dispersion coefficient as a function of shear velocity	72
Estimation of Surface Shear Velocity. . . .	73
Surface shear velocity as a function of wind velocity	73
VI RESULTS AND DISCUSSION	74
Reaeration with no Wind	74
Reaeration as a function of velocity and depth	74
Reaeration as a function of the longitudinal dispersion coefficient	78
Reaeration as a function of shear velocity.	79
Characteristics of the prediction equations	85
Reaeration with Wind.	86
The developed formula	86
Advantages of the developed equation.	89
Applications of the equation.	90
Properties of the Water Surface	92

TABLE OF CONTENTS - Continued

<u>Chapter</u>		<u>Page</u>
	Roughness Effect on Reaeration Rates . .	103
	Dynamic effect of waves on reaeration	105
VII	SUMMARY AND CONCLUSIONS	107
	Summary.	107
	Conclusions.	108
	Reaeration with no wind.	108
	Reaeration with wind	109
	Properties of the water surface. . .	111
	The effect of surface roughness on reaeration.	111
	BIBLIOGRAPHY	113
	APPENDIX - TABLES	119

LIST OF TABLES

<u>Table</u>		<u>Page</u>
1	REAERATION WITH NO WIND	120
2	REAERATION WITH WIND.	121
3	WAVES DATA.	122
4	SUMMARY OF REAERATION WITH WIND	123

LIST OF FIGURES

<u>Figure</u>		<u>Page</u>
1	Velocity profile in the water.	40
2	Forces on moving water with wind	42
3	Distribution of wind driven currents in a standing water	44
4	Schematic diagram of the CSU wind-water tunnel	48
5	The CSU wind-water tunnel.	51
6	Calibration of capacitance wave gauge.	51
7	Characteristics of roughness meshes.	52
8	Sketch of capacitance probe.	54
9	Hydraulic circuit of the sample flow and fitting of the sensor.	57
10	The sampling probe	58
11	Methods of sampling and connections.	59
12	Calibration of Beckman's oxygen analyzer	61
13	Location of sections in the flume.	69
14	Example of reaeration coefficient determination.	71
15	Reaeration coefficient as a function of $U/R^{3/2}$.	76
16	Observed versus predicted values of k_2	77
17	Reaeration coefficient as a function of D_L/R^2 . .	80
18	Observed versus predicted values of k_2	81
19	Observed versus predicted values of k_2	83
20	Reaeration coefficient as a function of u_{*b}/R . .	84
21	Reaeration coefficient as a function of $R_{sh}(u_{*c}/h)$	87
22	Observed versus predicted values of k_2	88

LIST OF FIGURES - Continued

<u>Figure</u>		<u>Page</u>
23	Variation of wave height with fetch and air velocity.	93
24	Variation of wave length with fetch and air velocity.	94
25	Variation of wave frequency with fetch and air velocity.	96
26	Variation of the surface shear velocity, wave height, and the reaeration coefficient with fetch.	98
27	Variation of wave height and wave frequency with the surface shear velocity at a fixed position in the flume	99
28	Observed wave speed compared with theoretical .	101
29	Observed wave speeds as compared with other investigators	102
30	Variation of reaeration coefficient with wave height	104

LIST OF SELECTED SYMBOLS

<u>Symbol</u>	<u>Definition</u>	<u>Dimension</u>	<u>Units</u>
a	Radius of pipe	L	---
A	Area of gas-liquid interface	L^2	---
b	Width of channel	L	ft
\bar{c}_e	Measured wave speed relative to fixed reference system	L/T	ft/sec
c_t	Theoretical wave speed based on wave length	L/T	ft/sec
C_A	Ratio of actual surface area to projected surface area	-	---
C_i	Concentration of gas in interface	M/L^3	---
C_L	Concentration of gas in main body of liquid	M/L^3	---
C_s	Saturation concentration of gas in liquid	M/L^3	---
C_t	Concentration of oxygen at time t	M/L^3	---
D	Dissolved oxygen deficit	M/L^3	mg/l
D_o	Initial dissolved oxygen deficit	M/L^3	---
\bar{D}_y	Turbulent diffusion coefficient, averaged over depth	L^2/T	---
D_L	Longitudinal mixing coefficient	L^2/T	ft ² /sec
D_m	Molecular diffusion coefficient	L^2/T	---
D_T	Effective turbulent diffusion coefficient	L^2/T	---
E	Energy dissipation per unit mass of fluid	L^2/T^3	---
f	Wave frequency	$1/T$	1/sec
$f(t)$	Relative part of surface film having ages between t and $t + dt$	-	---

LIST OF SELECTED SYMBOLS - Continued

<u>Symbol</u>	<u>Definition</u>	<u>Dimension</u>	<u>Units</u>
F	Froude number	-	---
g	Acceleration due to gravity	L/T^2	ft/sec ²
\bar{H}	Average wave amplitude	L	in
h	Normal depth, i.e., depth with uniform flow	L	ft
K	Henry's law constant	-	---
k	Wave number	1/L	---
k_2	Reaeration coefficient - base 10	1/T	1/sec
K_L	Overall transfer coefficient through liquid film	L/T	---
K_y	Eddy diffusivity or turbulent mass transfer coefficient in the y-direction	L^2/T	---
K_1	BOD rate constant - base e	1/T	
K_2	Reaeration coefficient - base e	1/T	---
l	Prandtl mixing length	L	---
L	Biochemical oxygen demand	M/L^3	
L'	Thickness of liquid surface film	L	---
L_o	Initial biochemical oxygen demand	M/L^3	---
m	Mass of solute gas	M	---
N	Rate of mass transfer, during time t, per unit surface area	M/TL^2	---
p	Partial pressure of oxygen	M/LT^2	
P	Air pressure in tunnel above	M/LT^2	lb/ft ²
Q	Volumetric rate of discharge of water in the channel	L^3/T	ft ³ /sec
r	Rate of surface renewal	1/T	---
R	Hydraulic radius	L	ft
R_{sh}	Shear Reynolds number	-	---

LIST OF SELECTED SYMBOLS - Continued

<u>Symbol</u>	<u>Definition</u>	<u>Dimension</u>	<u>Units</u>
s	Jeffreys' sheltering coefficient	--	---
S_o	Slope of channel	--	---
S_e	Slope of energy gradient	--	---
S_c	Pressure adjusted channel slope = $S_o + \frac{1}{\rho g} \frac{dP}{dx}$	--	---
t	Time	T	sec
T	Temperature	--	°C
u_*	Shear velocity in a wide, open channel as $\sqrt{\tau_o/\rho}$ or $\sqrt{ghS_e}$	L/T	ft/sec
u_{*D}	Bed shear velocity, by side wall correction method	L/T	ft/sec
u_{*C}	Shear velocity defined as $\sqrt{ghS_c}$	L/T	ft/sec
u_{*S}	Surface shear velocity defined as $\sqrt{\tau_s/\rho}$	L/T	ft/sec
U	Average water velocity	L/T	ft/sec
U_s	Water-surface velocity	L/T	fps
$\sqrt{\overline{v'^2}}$	Root-mean-square velocity fluc- tuation in the y-direction	L/T	---
V	Reference air velocity	L/T	ft/sec
V_l	Local air velocity	L/T	ft/sec
x,y,z	Distance in longitudinal, lateral and vertical directions	L	---
δ	Boundary layer thickness	L	---
ϵ_y	Eddy viscosity, or momentum transfer coefficient in y- direction	L^2/T	---

LIST OF SELECTED SYMBOLS - Continued

<u>Symbol</u>	<u>Definition</u>	<u>Dimension</u>	<u>Units</u>
κ	von Karman turbulence coefficient	--	---
$\bar{\lambda}$	Average wave length	L	in
ν	kinematic viscosity	L^2/T	---
ρ	Mass density of water	M/L^3	---
ρ_a	Mass density of air	M/L^3	---
σ	Surface tension	M/T^2	---
τ_b	Average shear stress on flume bottom	M/LT^2	---
τ_d	Boundary shear stress acting on the body of water	M/LT^2	---
τ_s	Average shear stress on water surface	M/LT^2	
τ_w	Shear stress due to the channel side walls	M/LT^2	

Chapter I

INTRODUCTION

Stream Reaeration

Absorption of atmospheric oxygen by natural bodies of water is of major importance. Through atmospheric reaeration a stream can recover its oxygen resources once they have been depleted by bacterial decomposition of organic impurities, such as municipal sewage and industrial wastewater. To achieve successful pollution control, one must know accurately this reaeration capacity. The evaluation of the natural purification rate of a stream and therefore its waste assimilative capacity are the necessary basis for accurate determination of waste treatment requirements in any specific situation, and are thereby the principal requirements for accurate evaluation of the costs of pollution control. The importance in determining waste treatment requirements and associated costs makes the development of a practical method for predicting oxygen absorption rate a significant contribution to the waste disposal problem.

Wind-Waves and Reaeration

For an undisturbed body of water, where the only forces acting on its free surface are a constant gravity field and a uniform atmospheric pressure, the body is stagnant and the water surface is level. However, there are other forces that will tend to change this equilibrium position. Some

of these natural forces are: wind, rain, earthquake, and change in atmospheric pressure.

When wind passes over a leveled water surface, a current develops in the upper layer of the water in the direction of the wind. If the wind is of sufficient intensity, waves will form on the water surface; their fluid mechanical behavior has been widely studied. However, very few quantitative investigations have been made of the effect of waves on interfacial mass transfer.

In turbulent water, reaeration is a physical process that takes place by the combining effects of absorption of gas molecules into the surface of the liquid and the physical mixing of the water. In a stagnant body of water, the reaeration is very slow because it depends on the molecular diffusion of the dissolved gas molecules into the surface film, and that is a slow process. But when wind blows over the water surface a substantial increase in rate of reaeration takes place. Two reasons could be given for this increase. First, when waves are formed there is an increase in the interfacial area. Second, and more important, in this turbulent flow regime, at the surface, an energetic and random agitation of the fluid takes place. This agitation brings about a continuous interchange of the surface water layer by fluid from the interior of the water and thereby greatly increases both the net rate of entry of gas molecules at the water surface and the subsequent rate of diffusion throughout the whole volume. This movement by

turbulent diffusion of the gas molecules into and through the interface is much faster than that of molecular diffusion.

For the process of reaeration, without wind, in streams and rivers, many models have been reported in the literature; many of these models were tested by both laboratory and field investigations. A few quantitative studies have been also reported on the effect of small ripples, forming in falling liquid films, on the interfacial mass transfer. Yet, no systematic experiments have been performed that were designed to test quantitatively how much of the increase in the reaeration would be due to the action of wind on water in open channels.

Research Objectives

Briefly stated, the goals of this investigation were to provide laboratory data and develop a practical method to predict the rate of reaeration in natural streams and rivers with wind blowing over the water surface. The experimental data were obtained in a laboratory flume with wind blowing over the surface of water flowing at normal depth.

More specifically, the goals were to:

- a. Explain the transfer mechanism of oxygen from the air to flowing streams and rivers.
- b. Develop a practical method for estimating oxygen uptake rates in streams and rivers, with wind blowing.

c. A subsidiary objective was to test some of the reaeration coefficient, with no wind blowing over the water surface.

To accomplish these objectives the following research procedure was used.

Research Procedure

The research procedure undertaken and its presentation in this dissertation is as follows:

a. Examination of the models used by earlier authors for explaining the gas absorption process, which is done in Chapter II.

b. Development of a theoretical relationship between gas absorption and the wind intensity, given in Chapter III.

c. Development and presentation of the experimental procedures used for measuring oxygen absorption rates and the water surface elevations in an open channel with wind blowing over the water surface, given in Chapter IV.

d. Presentation, analysis and discussion of the experimental data, given in Chapters V, VI and VII.

The experiments were conducted in the Wind-Water Tunnel, Fluid Dynamics and Diffusion Laboratory, Colorado State University.

Chapter II

REVIEW OF LITERATURE

This chapter begins with an examination of earlier theoretical approaches to the gas transfer processes, and a review of works on stream reaeration, which are relevant to the problem at hand. Then a review of methods used for predicting the longitudinal dispersion coefficient, in a two-dimensional uniform open channel flow, is outlined. And finally, an explanation is given of the interaction processes between the wind and the water surface.

Theories of Gas Absorption Mechanism

Many theories of gas absorption are reported in literature. These are presented in this section, and some of these ideas will be adopted in the theoretical development of this work.

Basic equations of molecular diffusion - For gases which do not react chemically with water to any great extent, the mass of the gas, which will dissolve in water at a given temperature, is directly proportional to the partial pressure of the gas in contact with the water. Under conditions of equilibrium and constant temperature, this relationship, called Henry's law, may be expressed by the equation:

$$C = Kp \quad (1)$$

in which C is the concentration of gas in the water, at equilibrium; p is the partial pressure of the gas, and K is a constant.

When water which contains less than a saturation concentration of oxygen, is exposed to air, oxygen is immediately absorbed in the surface monolayer of water. This thin layer of water is instantaneously saturated with dissolved oxygen. As long as this saturated layer remains on the surface, the oxygen molecules can penetrate into the water only by the process of molecular diffusion. In the case of a stagnant body of water, the rate of absorption is governed by the rate that oxygen is transferred, by molecular diffusion, into the interior of the fluid throughout the depth, as given by Fick's law of diffusion:

$$\frac{\partial m}{\partial t} = - D_m \frac{\partial C}{\partial y} \quad (2)$$

where $\partial m / \partial t$ is the rate of mass transfer, by diffusion, per unit area; $\partial C / \partial y$ is the concentration gradient in the direction perpendicular to the cross section area; and D_m is the coefficient of molecular diffusion (diffusivity).

For one-dimensional diffusion (in the y -direction)

$$\frac{\partial m}{\partial t} = \int_y \frac{\partial C}{\partial t} dy \quad (3)$$

then from 2, Fick's second law can be deduced

$$\frac{\partial C}{\partial t} = D_m \frac{\partial^2 C}{\partial y^2} \quad (4)$$

This equation states that the rate of change of concentration of the dissolved gas at any point y is proportional to the rate that the concentration gradient, $\partial C / \partial y$, is changing in the y -direction.

Equation (4) is for the case of unsteady state transfer; and knowing the boundary conditions, it could be applied for any particular case of molecular diffusion.

Equations (3) and (4) are valid for a quiescent body of water, and they have little application to stream flow conditions. However, they are still of great importance, because of the wide belief that the main resistance to mass transfer occurs at the gas-liquid interface, where the transfer process is by molecular diffusion.

The oxygen sag equation - Adney and Becker (1919) have assumed that oxygen absorption into water is a first order kinetic process; i.e., the rate of absorption is proportional to the oxygen deficit. This process can be expressed by the following differential equation:

$$\frac{dD}{dt} = - K_2 D \quad (5)$$

where D is the oxygen deficit below saturation (the difference between the dissolved oxygen saturation value, C_s , and the concentration of oxygen, C_t , at time, t); and K_2 is the reaeration rate constant.

Equation (5) could be deduced by integrating Equation (4) over the depth, i.e.,

$$\frac{1}{h} \frac{\partial}{\partial t} \int_0^h C dy = \frac{1}{h} \int_0^h \frac{\partial}{\partial y} (D_m \frac{\partial C}{\partial y}) dy$$

or

$$\frac{d\bar{C}}{dt} = \frac{1}{h} [D_m \frac{\partial C}{\partial y}]_0^h ,$$

the boundary conditions requires that $[D_m \frac{\partial C}{\partial y}]_0 = 0$ and $[D_m \frac{\partial C}{\partial y}]_h = K_L (C_s - \bar{C})$, thus, in terms of deficit where $D = C_s - \bar{C}$,

$$\frac{dD}{dt} = - \frac{K_L}{h} D = - K_2 D.$$

The solution to Equation (5) can be written

$$\ln \frac{D_1}{D_2} = K_2 (t_2 - t_1) = K_2 t_0$$

from which

$$K_2 = \frac{\ln D_1 - \ln D_2}{t_0}$$

or

$$k_2 = \frac{\log D_1 - \log D_2}{t_0} \quad (6)$$

where $K_2 = 2.303 k_2$; D_1 is the oxygen deficit at station 1 at any time t_1 ; D_2 is the dissolved oxygen deficit at station 2 at any time t_2 ; and t_0 is the time of flow between stations 1 and 2.

For Equation (6) it is assumed that the reaeration coefficient is independent of the dissolved oxygen concentration at the time of measurement.

The two film theory - Lewis and Whitman (1923, 1924) postulated that, at the interface of a gas and a turbulent liquid, there are two stagnant thin films of gas and liquid. Through these films the gas must pass by molecular diffusion. Below them the concentration of the dissolved gas is uniform. Conditions at the interface are gas diffusing through either film must also diffuse through the other and that there is no accumulation of gas at the interface beyond that corresponding to saturation. This steady state rate of transfer across the film could be expressed by

$$\frac{dm}{A dt} = D_m \frac{C_i - C_L}{L'} = K_L (C_i - C_L) \quad (7)$$

from which the rate of change of concentration of oxygen in the main body of the liquid is

$$\frac{dC_L}{dt} = K_L \frac{A}{V_o} (C_i - C_L) \quad (8)$$

In the above two expressions, dm/dt is the rate of mass transfer of solute dissolved gas; D_m denotes the molecular diffusivity of the gas in the liquid; C_i is the concentration of gas at the interface; C_L denotes the concentration of gas in main body of liquid; A is the area of gas-liquid interfaces, V_o refers to the volume of the liquid; K_L is the overall gas transfer coefficient which is commonly referred to as the liquid film coefficient, $K_2 = K_L/h$, and L' denotes the thickness of liquid surface film.

In spite of the greater thickness of the gas film, it offers less diffusion resistance to slightly soluble gases, such as oxygen, than does the liquid film. For this slightly soluble gas, there is practically no concentration gradient in the gas film. Then, the concentration at the interface could be determined from Henry's law, Equation (1), or $C_i = C_s$. Equation (8) then becomes

$$\frac{dC_L}{dt} = K_L \frac{A}{V_O} (C_s - C_L) \quad (9)$$

The stagnant film theory, Equation (7), predicts that the overall mass transfer coefficient varies as the first power of the diffusivity, but the data of Sherwood and Holloway (1940) for a packed tower, indicate that it varies as the square root of the diffusivity. The main objection to the stagnant film theory is the assumption of the steady-state rate of mass transfer, where as in a turbulent liquid the surface film is being continuously replaced by liquid from below. According to Lewis and Whitman (1924), the theory has its most precise application when conditions on both sides of the air-water surface are turbulent; this and the assumption of the stagnant film imply that close to the surface, in the viscous sublayer, turbulence eddies becomes so small that the mass transferred by molecular viscosity exceeds that transferred by turbulent eddies. However, because the molecular diffusion coefficient is much smaller than the kinematic viscosity, the turbulent eddies still

transfer substantially more solute gas than molecular diffusion.

The penetration theory - A more realistic notion of the process of gas absorption, and one that predicts that K_L , for the limiting case of short time of exposure, is proportional to $\sqrt{D_m}$, was introduced by Higbie (1935). Higbie considered the mass transfer as an unsteady-state process in which the concentration of solute at any place in the film is controlled by penetration, by molecular diffusion, of the dissolved gas molecules into the liquid film and by bodily transport of the molecules owing to the bulk motion of the film. He used, then, the word film to describe the entire liquid layer, but not the hypothetical stagnant film of the Whitman theory.

Higbie's derivation is based on the following assumptions: (1) the film is in laminar motion, (2) the surface of the film is moving at a uniform velocity in the horizontal direction, (3) the interfacial concentration has a constant value C_s , and (4) the effect of diffusion in the direction of flow is negligible. With these assumptions, the penetration theory can be valid only for times of exposure so short and for turbulence so low that the diffusing gas does not penetrate into those parts of the liquid which have a velocity appreciably different from that at the surface.

According to Higbie the average rate of mass transfer during the time t_s is

$$N = 2(C_s - C_L) \sqrt{D_m / \pi t_s} \quad (10)$$

with a corresponding liquid film coefficient

$$K_L = \frac{N}{(C_s - C_L)} = 2\sqrt{D_m / \pi t_s} \quad (11)$$

Danckwerts' modified penetration theory: Surface

Renewal Theory - Danckwerts (1951) modified the model of Higbie by introducing a factor, r , which he defined as the frequency of replacement of the liquid film. In a turbulent flow regime, liquid elements at the surface, which have been exposed to the gas for varying lengths of time, are replaced by other elements arising from the turbulent movements of the body of the liquid. Any part of the surface liquid film may be replaced at any time after its creation by the action of turbulence. Because of the random nature of the turbulence, there is no correlation between the age of an element and its chance of being replaced. The transfer coefficient for the entire surface must then depend upon the distribution of ages within the film. Danckwerts defined this distribution by

$$f(t) = re^{-rt} \quad (12)$$

where r is the mean rate of surface renewal.

The rate of absorption into the fractional portion of the area, $re^{-rt} dt$, having ages between t and $t + dt$, is found from Equation (10) to be $(C_s - C_L)re^{-rt} \sqrt{D_m / \pi t} dt$.

The mean rate of absorption per unit area of turbulent surface, having age, t , is

$$\begin{aligned} N &= (C_s - C_L) \sqrt{D_m} \int_0^{\infty} \frac{re^{-rt}}{\sqrt{\pi t}} dt \\ &= (C_s - C_L) \sqrt{D_m r} \end{aligned} \quad (13)$$

$$\text{from which } K_L = \frac{N}{C_s - C_L} = \sqrt{D_m r} \quad (14)$$

Dobbins (1956), using a slightly different model for film penetration, found the following expression for K_L

$$K_L = \sqrt{D_m r} \coth \sqrt{\frac{rL'^2}{D_m}} \quad (15)$$

in which L' is the film thickness. This equation reduces to Danckwerts' equation ($K_L = \sqrt{D_m r}$) as the argument of \coth becomes 3 or greater and approaches the stagnant film equation ($K_L = D_m/L'$) as the renewal rate, r , approaches zero.

The Kishinevski theory - Kishinevski (1955), abandoned the concept of a laminar surface film, and concluded that mass transfer across the surface layer is determined by turbulent diffusion. The experimental results of Kishinevski and Serebnyansky (1956) shows that, although the molecular diffusion coefficient is much higher for hydrogen than for nitrogen or oxygen, the mass transfer coefficient is the same for all these three gases. This led them to conclude, in the experimental conditions they

used, that molecular diffusion plays no essential part in the mass transfer.

Kishinevski presented the following equation for the absorption coefficient

$$K_L = \frac{2}{\sqrt{\pi}} \sqrt{D_T r} \quad (16)$$

where D_T is the effective coefficient of diffusion including both turbulent, D_{turb} , and molecular diffusion, D_m .

Dobbins (1964) findings contradicted those of Kishinevski, because he found the absorption coefficient, K_L , to be dependent on the diffusivity of the gas, over a wide range of turbulent conditions.

The effect of molecular diffusivity on the oxygen absorption process is usually expressed by showing how the value of K_L varies with D_m raised to an exponent, n .

$$K_L \propto D_m^n \quad (17)$$

where in the two film theory, n takes the value of unity, while the theories of Higbie and Danckwerts' give values of 0.5. The work of Dobbins (1964) shows that the value of n can vary from 1.0 to 0.5, while Kishinevski shows that it can fall to zero with conditions of high turbulence.

The concept of a single stagnant film constituting the entire resistance, to interphase transfer of material, is an oversimplification of the situation, and much of the

resistance may be in the eddy zone or "core" of the turbulent stream. Any analytical treatment of the whole process may be subject to serious error if it does not allow for the resistance to eddy diffusion which is a process fundamentally different in character from molecular diffusion. For example, Stirba and Hurt (1955) made some measurements of the absorption of pure gases in falling liquid films at low Reynolds numbers, and substantiated the findings of other investigators namely: that the mass transfer rates were many times greater than could have been predicted if molecular diffusion were the only transfer process.

The assumption of an effective turbulent diffusion coefficient, other than molecular diffusion, as the controlling factor in the interface mass transfer suggests itself for a better physical interpretation of the absorption process. However, Krenkel (1963), presented data which demonstrated that some mechanism other than either molecular or turbulent diffusion had a significant role in the gas absorption process. He concludes that " ... experiment evidence shows that some rate controlling factor, much less than turbulent diffusion, plays the significant role in gas transfer phenomenon."

If the rate of this interface mass transfer is a function of some effective diffusion coefficient, at the interface, and the rate of surface renewal, the reaeration rate constant could be defined as follows [Krenkel (1960), Krenkel and Orlob (1963), Thackston and Krenkel (1965)]

$$k_2 \propto \left(\frac{D_T}{\nu} \right) r \quad (18)$$

where D_T is an effective diffusion coefficient, at the interface; ν is the kinematic viscosity and r is the rate of surface renewal.

The Effect of Temperature on Reaeration

An increase in water temperature leads to an increase in the reaeration coefficient. Temperature influences the speed of the oxygen molecules in the water and in the air at the air-water interface; this will lead to an increase in the rate of molecular diffusion of oxygen at the interface and, thus, an increase in the reaeration coefficient.

The effect of temperature on reaeration can be represented by the following equation (O'Connor and Dobbins (1958))

$$k_2 = a_1 e^{b_1 T} \quad (19)$$

where a_1 and b_1 are constants, and T is the temperature.

Commonly, temperature effects are expressed by relating the rate of reaeration to a value at 20°C; then

$$k_{2(T)} = k_{2(20^\circ)} (e^{b_1})^{(T-20)} \quad (20)$$

H. W. Streeter (1935), G. A. Truesdel and Van Dyke (1958) reported, experimentally, that the reaeration rate varies with temperature according to the following equation

$$k_2(20^\circ) = k_2(T^\circ) (1.016)^{20-T} \quad (21)$$

Previous Work on Stream Reaeration

Streeter and Phelps (1925), in their classical studies of data derived from observations on the Ohio River, assumed that the biochemical oxygen demand in a stream was proportional to concentration of oxidizable matter remaining in the water; while the rate of reaeration, in accordance with the Adeney-Becker relation, Equation (5), was assumed to be directly proportional to the oxygen saturation deficit.

Based on these two processes, the following differential equation was formulated (e.g., Dobbins, 1964)

$$\frac{dD}{dt} = K_1 L - K_2 D \quad (22)$$

in which L and D represent the biochemical oxygen demand and the dissolved oxygen deficit, at time t , respectively. The equation implies that the rate of change in the dissolved oxygen saturation deficit is equal to the algebraic sum of the two independent rates, the rate of biochemical oxidation and the rate of atmospheric reaeration.

The above linear, first-order, differential equation was solved to give

$$D = \frac{K_1 L_0}{K_2 - K_1} [e^{-K_1 t} - e^{-K_2 t}] + D_0 e^{-K_2 t} \quad (23)$$

where L_0 and D_0 are the initial biochemical oxygen

demand and the initial dissolved oxygen deficit, respectively; K_1 is the deoxygenation coefficient, base e , and K_2 is the reaeration coefficient, base e .

Equation (23) has been used as the basis for calculating reaeration coefficients, for various reaches of the Ohio River, from determination of biochemical oxygen demand and oxygen distribution. They formulated, empirically, the following relationship between the coefficient and the hydraulic properties of a given reach of a river

$$k_2 = \frac{a_1 U^{b_1}}{h^2} \quad (24)$$

where U is the mean stream velocity; a_1 and b_1 are constant; and h designates the mean depth of flow. Because the empirical constants a_1 and b_1 depend on the hydraulic and physical properties of each reach, the above equation is of limited practical application.

O'Connor and Dobbins (1958) reported a correlation of the reaeration coefficient with the turbulence parameters of the stream, and the field application of that correlation. In their theoretical approach they defined the reaeration coefficient in terms of the rate of surface renewal, r , where they assumed this surface renewal to be the ratio of the vertical rms velocity fluctuation at the surface, $\sqrt{\bar{v}'^2}$, to the Prandtl mixing length, l , i.e.,

$$r = \frac{\sqrt{\bar{v}'^2}}{l} \quad (25)$$

For streams having a significant vertical velocity gradient, the following formula for nonisotropic turbulence conditions was developed:

$$K_2 = 480 \frac{D_m^{1/2} S_e^{1/4}}{h^{5/4}} \quad (26)$$

and for relatively deep channels, they assumed there is no pronounced velocity gradient and hence, the turbulence may approach an isotropic condition, the equation takes the form

$$k_2 = 127 \frac{(D_m U)^{1/2}}{h^{3/2}} \quad (27)$$

In the above two equations, D_m is the coefficient of molecular diffusion; S_e is the slope of the energy gradient; U is the mean velocity of flow; and h is the normal depth of flow.

The Chezy coefficient was used as criterion of the state of turbulence. Isotropic turbulence was assumed for Chezy coefficients greater than 17, and nonisotropic turbulence for less than 17. When the Chezy coefficient has a value of 14.2, the reaeration coefficients calculated, using both equations, are equal.

O'Connor and Dobbins concluded their work by comparing the coefficients, k_2 , observed from the river surveys and those computed from their proposed formulas. They presented a surprisingly good agreement between

the two values in spite of the criticisms that were made, by A. N. Diachishin (1958) and E. A. Pearson (1958), to the development and the applications of the two formulas.

Churchill et al. (1962), reported a field study of 30 selected stream reaches in the Tennessee Valley, where efforts were made in gathering field data on stream reaeration rates with the water being free of pollution. They used dimensional analysis in forming different equations relating k_2 with various hydraulic parameters of the stream, where the methods of statistical correlation techniques was used in determining the coefficients of these various equations. They recommended the following equation, to predict the reaeration rate from the average velocity, depth and temperature of the water

$$k_2(T^\circ) = 5 \frac{U}{R^{5/3}} (1.0241)^{T-20} \quad (28)$$

where U denotes the mean velocity; R is the hydraulic radius; and T is the water temperature in degrees centigrade.

They also concluded that inclusion of other flow variables, such as channel roughness and energy slope would not greatly increase the accuracy of the predicted values.

Krenkel (1960) and Krenkel and Orlob (1963) introduced a rational concept where they assumed that the rate of reaeration is proportional to the rate of surface

renewal, r , and that r being proportional to the longitudinal dispersion coefficient, D_L , i.e., $r \propto D_L/h^2$. Krenkel, adopting the concept that $k_2 \propto r$, has, presumably, assumed that for a laminar flow regime at the interface, the diffusion coefficient D_T in Equation (18) is proportional to v . He has also reported fifty-eight values of k_2 and corresponding values for D_2 and proposed the empirically derived equation

$$k_2 = 4.3 \times 10^{-5} D_L^{1.15} h^{-1.95} . \quad (29)$$

Krenkel adopted the longitudinal dispersion coefficient, D_L , and not the vertical eddy diffusivity, k_y , because the eddy diffusivity is a local parameter and it may vary from point to point in a nonuniform flow and because of its limited practical application. Krenkel further stated that "the longitudinal mixing coefficient, on the other hand, reflects the mixing properties of the entire stream section and indicates the effect of turbulence in the section on mixing of absorbed surface layers of oxygen into the main body of the stream. Moreover, determination of the longitudinal mixing coefficient is practical and relatively economical."

Krenkel also reported that the reaeration coefficient was directly proportional to the energy expenditure per unit mass of fluid, E , where he showed

$$k_2 = 1.14 \times 10^{-4} E^{.41} h^{-.66} . \quad (30)$$

For open channel flow, the energy expenditure per unit mass can be expressed as (Krenkel)

$$E = U S_e g \quad (31)$$

where S_e is the slope of the energy gradient.

Dobbins (1956) presented a mathematical model explaining the process of reaeration, where he assumed that the surface film is always present, in a statistical sense, but the liquid in this interfacial film is being continuously replaced by liquid from the main body. This concept combined with the use of basic transfer Equation (3) and the age distribution function of Danckwerts, Equation (12), led to the formation of Equation (15), where

$$K_L = \sqrt{D_m} r \coth \frac{r L'^2}{D_m} \quad (15)$$

Later, Dobbins (1964), modified the above equation by relating r to L' , and substituting into Equation (15) gave:

$$\frac{K'_L (C_4)^{3/2}}{C_A \sqrt{C_5 D_m}^\alpha} = \coth \sqrt{\frac{C_5 \psi}{C_4 D_m}} \quad (32)$$

in which

$$\alpha = \frac{\rho (vE)^{3/4}}{\sigma}$$

$$\psi = \frac{\rho v^{9/4} E^{1/4}}{\sigma}$$

$$C_A = 1.0 + 0.3 F^2$$

$$K'_L = C_A K_L$$

and
$$C_4 = 0.65 + 1500 [(\nu^3/E)^{1/4}/h]^2 .$$

In the above expressions, C_A is the ratio between the actual surface area and the projected surface area; F is the Froude number; K'_L is the apparent exchange coefficient; ρ is the mass density; ν denotes the kinematic viscosity; σ is the surface tension; and E denotes the energy expenditure per unit mass of fluid, as defined in Equation (31). C_5 , in Equation (32), is a constant with a value of 14.3. Dobbins obtained this value experimentally with a laboratory mixer, and suggested the same value would be applied for streams.

Thackston (1966), based his theoretical development on a premise that the reaeration rate constant is proportional to some function of surface renewal and inversely proportional to some function of the depth. Then, he extended this premise by adopting the concept, which was first originated by Krenkel, that the vertical eddy diffusion coefficient, K_y , as an indicator of r . Finally, Thackston, formulated the following expression for k_2

$$k_2 \propto \frac{K_y}{h^2} . \quad (33)$$

To find an expression for K_y , Thackston, in his development, assumed that the Reynolds analogy is valid, according to which K_y and the eddy viscosity ϵ_y are used interchangeably. The analogy has been confirmed experimentally by Kalinske and Pien (1944), G.I. Taylor (1954), and Al-Saffar (1964). Also V.A. Vanoni (1946) shows distribution of both ϵ_y and K_y to confirm that they are nearly equal.

Thus, Thackston took $\bar{\epsilon}_y$, the average of eddy viscosity over depth, as a measure of the average rate of vertical mixing of mass, and this rate is one of the controlling factor in reaeration.

To find an expression for $\bar{\epsilon}_y$, Thackston used the von Karman universal velocity distribution for open channel flow,

$$U_{(y)} = U + \frac{u_*}{\kappa} \left(1 + \ln \frac{y}{h} \right) \quad (34)$$

in which κ represents von Karman constant, usually taken as equal to 0.4; U is the average water velocity; u_* is the shear velocity, and $U_{(y)}$ is the velocity at a distance y from the bottom.

Using the above velocity distribution, the following expression for ϵ_y could be derived, Sayre (1968),

$$\epsilon_y = \kappa u_* y \left(1 - \frac{y}{h} \right) . \quad (35)$$

The expression for $\bar{\epsilon}_y$ was obtained by integrating the above equation with respect to y and dividing by the depth h ,

$$\bar{\epsilon}_y = \frac{\kappa}{6} h u_* . \quad (36)$$

Combining Equations (33) and (36), the following equation was obtained

$$k_2 = C \frac{u_*}{h} \quad (37)$$

To verify Equation (37), Thackston prepared experiments using a 60-foot long, two-foot wide, recirculating flume. The final equation describing his laboratory data was

$$k_2 = 0.000215 \frac{u_*}{h} \quad (38)$$

To compare his observations to those of Krenkel (1960), Thackston used the following relationship,

$$D_L = C h u_* \quad (39)$$

in defining the reaeration rate constant, k_2 , in terms of the longitudinal dispersion coefficient, D_L , and the water depth, h , this relationship is

$$k_2 = C \frac{D_L}{h^2} \quad (40)$$

Thackston, based on data obtained in his study, suggested the following equation for k_2 ,

$$k_2 = 0.000015 \frac{D_L}{h^2} \quad (41)$$

The corresponding equation from the data of Krenkel was

$$k_2 = 0.000052 \frac{D_L}{h^2} \quad (42)$$

The k_2 values of Krenkel are about 3.5 times those of Thackston. Both researchers used recirculating flumes which were essentially identical except for channel width. The same channel roughness was applied, but Krenkel used a 1-ft wide channel while Thackston used a 2-ft wide channel. This discrepancy, in the k_2 values, was recognized by Thackston (1966), who stated:

"The original data of Krenkel were examined carefully, and several values of k_2 were recomputed independently, using the oxygen saturation values of Churchill. No mistakes in procedure or mathematics were found, and the change in oxygen saturation values had no appreciable effect. No explanation for the apparent difference can be found."

Unless the ratio of width to depth were approximately the same in both cases, this difference could be attributed to some kind of wall effect.

Isaacs and Gaudy (1968), developed a rational prediction equation of k_2 , using dimensional analysis, and the constants in the equation were determined using observed data which were obtained under controlled experimental conditions. The experimental apparatus they used was a right circular cylindrical torus-shaped tank. They placed inside

the tank two right circular cylindrical shell walls which were driven by two independently controlled variable-speed motors. They claimed that "This arrangement permitted attainment of a velocity profile representing a desired experimental stream condition."

In developing a prediction equation of k_2 , they proposed that k_2 is a function of the following controlling variables

$$k_2 = f(U, h, D_m, \nu, g) \quad (43)$$

Using the Buckingham theorem along with dimensional analysis theory, the following equation was formed,

$$k_2 = C \left[\frac{D_m^{(1-d_1)}}{\nu^{(a_1-d_1)}} \right] \left(\frac{1}{g^{b_1}} \right) U^{(a_1+2b_1)} h^{(a_1-b_1-2)} \quad (44)$$

in which a_1, b_1, C, d_1 are constants.

They assumed that for constant experimental conditions of temperature and pressure, the group

$$C \left[\frac{D_m^{(1-d_1)}}{\nu^{(a_1-d_1)}} \right] \frac{1}{g^{b_1}}$$

be a constant, C' . Then they expressed Equation (44) as

$$k_2 = C' U^m h^p \quad (45)$$

Least squares analysis performed on the 52 experiments yielded the predictive equation for k_2 at 20°C

$$k_2 = 3.053 \frac{U}{h^{3/2}} \quad (46)$$

where k_2 is in day^{-1} ; U is in feet per second; and h is in feet.

When the natural stream data of Churchill et al. (1962) are used to evaluate the constants in Equation (45), the following equation is obtained,

$$k_2 = 4.020 \frac{U}{R^{3/2}} \quad (47)$$

The difference between the values of the constants, 3.053 and 4.020, can be attributed to the difference in channel geometry.

Summary on stream reaeration - Churchill et al. (1962), Krenkel and Orlob (1963), Thackston (1966), and Isaacs and Gaudy have all presented empirically derived equations relating the reaeration rate constant to various hydraulic variables.

O'Connor and Dobbins (1958), and Dobbins (1964), on the other hand, have developed theoretical relationships between the reaeration coefficient and the physical parameters of streams and channels. In evaluating these theoretical relationships, M. Owens et al. (1964) stated "... although these equations were derived by a rational procedure, there is a degree of empiricism in them." Using Dobbins equation, Equation (32), it is most difficult to evaluate the numerical values of the parameters involved,

and the results obtained using the O'Connor-Dobbins formulation, Equation (27), did not always agree with those observed in the laboratory and field studies, as noted by Diachishin (1958). The discrepancy could be attributed to some of the assumptions used in the development of the equation (Pearson, 1958).

Thus, only the models of Isaacs and Gaudy, Thackston, and Krenkel and the formulation of Churchill, will be examined further, by testing them against the experimental results from this investigation.

Prediction of Longitudinal Dispersion Coefficient

A subsidiary objective of this investigation was to test some of the models used by previous investigators for prediction of k_2 , with no wind blowing over the water surface. To accomplish this objective, an empirical equation is needed to predict the longitudinal dispersion coefficient, in a two-dimensional uniform open channel flow, using a measurable hydraulic parameters. In this section a rather brief theoretical consideration will be presented for predicting D_L .

Dispersion in open channel flow - G. I. Taylor (1954) presented the first important study of dispersion in turbulent shear flow, where he asserted that although the main mechanism of dispersion in shear flow is the variation in convective velocity within the cross section, the process

could be described by a one-dimensional Fickian diffusion equation,

$$\frac{\partial \bar{C}}{\partial t} + U \frac{\partial \bar{C}}{\partial x} = D_L \frac{\partial^2 \bar{C}}{\partial x^2} \quad (48)$$

where \bar{C} is the concentration averaged over the cross section; U is the cross-sectional average of the discharge velocity; x denotes the distance coordinate in the direction of flow; t represents the time, and D_L is the longitudinal dispersion coefficient.

The agreement between the Fickian theory and experimental observation is poor, according to Sayre and Chang (1966), they found a discrepancy between the time-concentration curves predicted by the Fickian diffusion equation and those observed by the laboratory investigations.

Taylor, using a 3/8-in.-diameter pipe, performed his analysis using an empirical velocity distribution and assumed that the turbulent eddy diffusivities were isotropic and could be defined by the Reynolds analogy, which states the equivalence of mass and momentum transfer. Taylor expressed the effective dispersion coefficient as,

$$D_L = 10.06 a u_* \quad (49)$$

where a is the pipe radius, and u_* represents the average shear velocity, $\sqrt{\tau_o/\rho}$, where τ_o denotes the wall shear and ρ is the fluid mass density.

Attempts have been made to extend Taylor's formula to open channels by substituting $2R$ for a in the above formula, in which R is the hydraulic radius.

Elder (1959), employed the von Karman-Prandtl logarithmic velocity distribution, which applies to both smooth and rough boundary conditions,

$$U(y) = U + \frac{u_*}{\kappa} \left(\ln \frac{y}{h} + 1 \right) \quad (50)$$

and the Reynolds analogy, arrived at the equation

$$D_L = \left[\frac{0.404}{\kappa^3} + \frac{\kappa}{6} \right] h u_* \quad , \quad (51)$$

where κ is the von Karman constant and h is the normal depth.

Sayre and Chang (1966), using a parabolic velocity distribution function,

$$U(y) = U + \frac{u_*}{\kappa} \left(-3 \frac{y^2}{h^2} + 6 \frac{y}{h} - 2 \right) \quad (52)$$

and the eddy diffusivity

$$\varepsilon_y = \frac{\kappa}{6} h u_* \quad ,$$

obtained the following expression for D_L ,

$$D_L = \left[\frac{0.457}{\kappa^3} + \frac{\kappa}{6} \right] h u_* \quad . \quad (53)$$

From their experimental data, Sayre and Chang reported a close agreement with Equation (51) for conditions of a logarithmic velocity distribution in the vertical and no lateral velocity gradient.

To verify Elder's application of Taylor analysis, Fischer (1967) reported his studies in flows which approximated the two-dimensional infinitely wide assumption. Experiments were done using channels with smooth bottoms and rough bottoms. The bed shear velocity with rough bottoms was obtained by application of the side-wall correction procedures given by Vanoni and Brooks (1957). Fischer presented the following empirical equation describing D_L , in a two-dimensional open channel flow with a rough bed,

$$D_L = 14.6 h u_{*b} \quad (54)$$

where u_{*b} denotes the bed shear velocity, by side wall correction method. The constant 14.6 represents the average values of D_L/hu_{*b} , for the runs with a rough bed.

The discrepancy among Equations (49), (51), and (53) is partly explained by the different velocity distribution assumed by each investigator. When Taylor's empirical velocity distribution is applied to an open channel, D_L/hu_* is approximately 11.7. However, if Elder's logarithmic distribution is applied to pipe flow, D_L/au_* is 5.84. Thus, the numerical difference between Taylor's result and Elder's is primarily caused by the velocity distribution. Equations (51) and (53) were obtained for

two-dimensional flow, with the only difference being the velocity distributions.

The Wind-Water Surface Interaction: Consequences

The interaction between wind and a water surface seems to have been considered in the literature from two points of view. In one, the water surface is regarded as a boundary of the same general nature as a solid boundary, with negligible velocity relative to that of the air, with the result of an interfacial shearing stress. From this point of view the principle problem is to determine the characteristic roughness length of the water surface.

On the other hand there is a growing body of literature (Eckart 1953; Ursel 1956; Phillips 1957; Miles 1957, 1959; Benjamin 1959) in which the problem of wave generation by wind is treated.

In this section a rather brief physical interpretation of the interaction between the wind and the water surface is presented. The processes of wind induced current and waves with their effect on the state of turbulence in the water is presented first. Then a method to estimate the shearing stress at the water surface is outlined.

Consequences: Turbulence - When wind blows over the surface of water, a tangential surface stress exists at the wavy interface and the air drags water along. Because of the non-vanishing viscosity of the water, this current

gradually deepens. The increase in water velocity, then, could be associated with an increase of turbulence, and with a corresponding increase in the turbulent diffusion. The increase of turbulent diffusion, due to the wind induced current, was observed by Masch (1963); he reported an exponential relationship between the surface current and the diffusion coefficient.

If the waves grow to the point where they start breaking, an increase in the turbulent intensity and energy dissipation will occur, especially near the surface. The turbulence near the surface is invigorated by the injection of sporadic energetic bursts of small-scale turbulence as the waves break. These bursts diffuse downward to some extent, decaying as they go. The energy supply from these motions can account for a substantial fraction of the total energy flux from the wind.

Estimation of the water surface shear stress -

Sinusoidal traveling waves formed on the water surface, due to wind, perturb the air flowing over them (in their direction of propagation) by undulations. These produce an air pressure distribution, which at any level is greatest over troughs and least over crests. Just above the water surface, the air is moving a little faster than the wave velocity, but, as it creeps forward from over a crest to over a trough, it is turned back by the higher pressure, moves down and returns toward the crest. Quantitatively, the downflow ahead of the crest must be such

as to provide a "vortex force," (an effective force per unit volume of fluid equal to its density times vorticity, ω , times the vertical velocity, v , and directed at right angles to the velocity), balancing the pressure gradient. This force, induced by the pressure difference between the wind-ward and lee side of waves, was called, Jeffreys (1925), a form drag. To this form drag, Jeffreys added the tangential drag, associated with skin friction, to give the total drag imposed on the water surface.

For air velocities below the critical velocity, no ripples will appear on the water surface and the skin friction is the predominant part of the drag. With an increase in air velocity, waves are generated and, consequently, an increase in friction results, as reported by Keulegan (1951) in his laboratory investigations. For high wind velocities, the drag will consist mainly of form drag, and could be expressed by the sheltering coefficient, s , of Jeffreys (1925) as

$$\tau_s = s \rho_a V^2 \frac{da}{dx}, \quad (55)$$

where ρ_a is the air mass density; V is the air velocity; a is the wave height, and da/dx represents the rate of change of wave height with respect to distance. Munk (1955), reported that da/dx is approximately proportional to V , and therefore,

$$\tau_s \propto \rho_a V^3.$$

According to Hidy and Plate (1966), for air velocities greater than 2 meter/sec,

$$\tau_s / \rho_a = u_{*s}^2 = 3.41 \times 10^{-4} V^3 \quad (56)$$

where u_{*s} and V are given in meter/sec. The above equation was deduced from a collection of data, determined using the wind-tunnel facility at Colorado State University.

From Equation (56) one can express the surface shear velocity as

$$u_{*s} = 0.0185 V^{3/2} \quad (\text{AIR}) \quad (57)$$

where u_{*s} and V are given in meter/sec.

Chapter III

THEORETICAL ANALYSIS

In this chapter a theoretical development of an equation for estimating oxygen absorption rates, applicable to natural streams and rivers with wind blowing, is presented.

Development of the Formula

The literature review on the theories of gas absorption, Chapter II, revealed that the assumption of an effective turbulent diffusion coefficient, at the interface, other than molecular diffusion, as the controlling factor in the interface mass transfer suggests itself for a better physical interpretation of the gas absorption process. Thus the physical model that will be adopted in the development of the equation consists of interfacial layers of water that absorb gas at a rate proportional to an effective diffusion coefficient at the interface, and that this surface water is then carried into the main body of liquid by the action of turbulence beneath the water surface. The rate of surface renewal, r , is assumed to be directly related to the state of turbulence occurring in the body of water. With these concepts, an expression for k_2 , Equation (18), was formulated [Krenkel (1960, Krenkel and Orlob (1963), Thackston and Krenkel (1965)] as follows

$$k_2 \propto \frac{D_T}{v} r \quad (18)$$

where D_T is an effective diffusion coefficient at the

interface; ν is the kinematic viscosity, and r is the rate of surface renewal.

Adopting the physical concept that the interfacial layers are carried into the main flow by the action of the vertical turbulence in the water, Krenkel considered the rate of surface renewal to be the turbulent diffusivity divided by the square of appropriate length scale. The channel depth was used as the most appropriate scale parameter. The resultant expression for k_2 was

$$k_2 = \frac{D_T}{\nu} \frac{\bar{D}_y}{h^2} \quad (58)$$

where \bar{D}_y is the average, over depth, of the turbulent diffusion coefficient of mass, and h is the depth of flow.

Estimation of \bar{D}_y - The Reynolds analogy, which states the equivalence of mass and momentum transfer, implies that the coefficient of turbulent diffusion of mass in the vertical direction, D_y , is approximately equal to the coefficient of turbulent diffusion of momentum in the vertical direction, ϵ_y . Thus, $\bar{\epsilon}_y$ can be considered as a measure of the average rate of vertical mixing of mass. Employing the logarithmic velocity distribution in a free open channel flow, an expression for $\bar{\epsilon}_y$ could be formulated [Sayre (1968), Al-Saffar (1964), Thackston (1966)]

$$\bar{\epsilon}_y = \frac{\kappa h}{6} \sqrt{\tau_b / \rho} \quad (36)$$

where κ denotes the von Karman constant; τ_b is the channel bottom shear stress, and ρ is the mass density of water.

In the water, with wind blowing over the surface, we assume a logarithmic velocity profile except in the thin layer at the surface. At the water surface there is a linear segment representing the drift current. A typical velocity profile (from Drake, 1967) is shown in Figure 1 which shows a comparison of this postulated profile and data from the Colorado State University Tunnel-Flume. The justification for the above shear flow come from the measurements of Vanoni (1946) in free water flow in channels and Plate and Goodwin (1965) in the wind water facility at Colorado State University.

Plate and Goodwin found that the major part of the velocity profile could be represented quite well by a logarithmic law of the form

$$\frac{U(y)}{u_*} = 6.06 \log \frac{y}{h} + C \quad (59)$$

where $U(y)$ is the water velocity at a distance y from the bottom; u_* is the water shear velocity, and C denotes a coefficient that characterizes the roughness of the channel floor.

In their evaluation of the above velocity distribution, Plate and Goodwin stated that

"The velocity distribution should extrapolate to reach the water surface drift velocity at $y/h = 1$. This would require a more rapid increase of the velocities near the water surface than can be obtained from an extension of the logarithmic distribution law. However, this increase is not evident in the data. Therefore, the effect of the

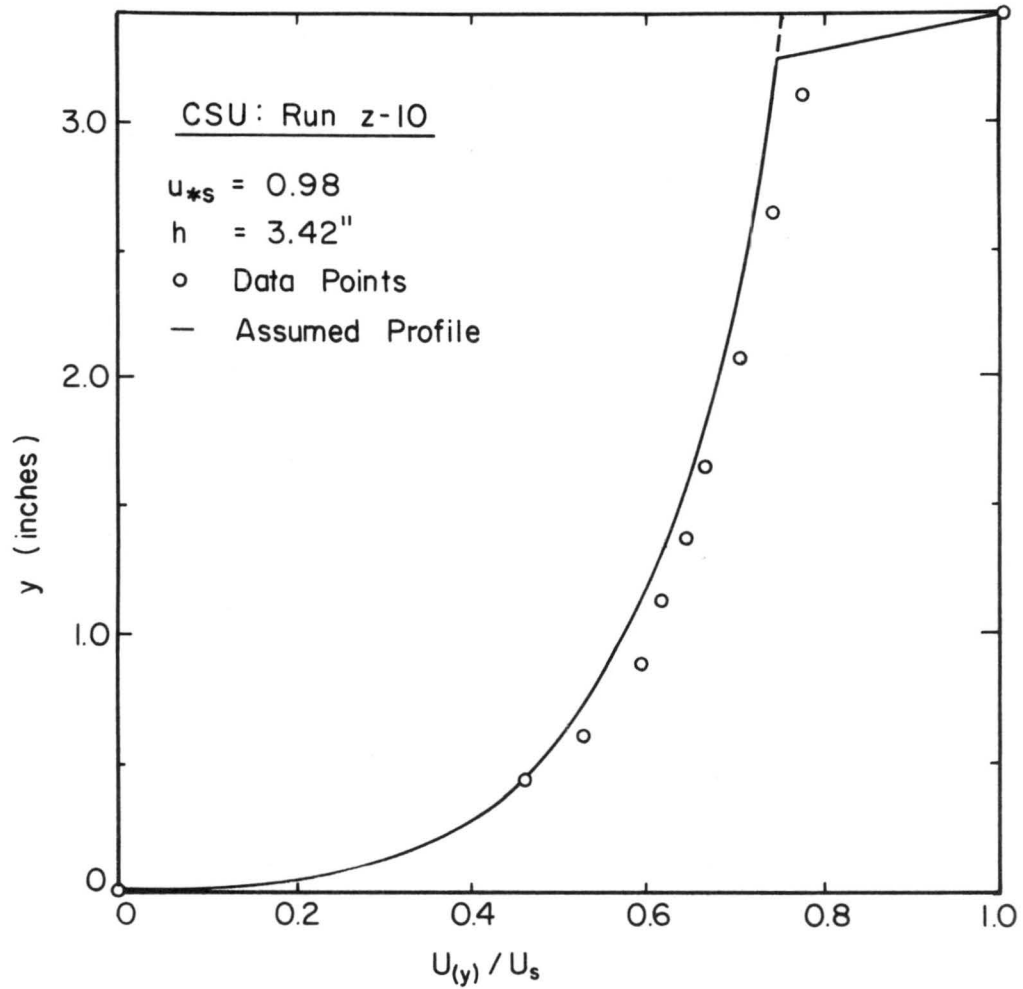


Fig. 1 Comparison of the Postulated Profile and Data from CSU [After Drake (1967)].

wind stress leads to a rapid increase of the velocities only within a thin layer close to the surface, unless of course, the trend is hidden in the scatter of the experimental data."

From their laboratory study of the influence of wind on open channel flow, Plate and Goodwin reported further that the shear velocity, u_* , in Equation (59) did not agree with the shear velocity calculated from the bottom shear stress, τ_b , but agreed with a shear velocity based on the net shear stress, τ_d , acting on the body of water. Thus, and in view of Equation (36), the average, across depth, of the momentum transfer coefficient, $\bar{\epsilon}_y$, can be expressed as

$$\bar{\epsilon}_y \propto \sqrt{\tau_d / \rho} \quad h \quad (60)$$

where τ_d denotes the net boundary-shear-stress acting on the body of water.

To determine the boundary shear stress, τ_d , the free body diagram, Figure 2, showing the forces on moving water with wind in a two-dimensional uniform channel flow, is used.

The force summation in the x-direction per unit width is:

$$\begin{aligned} \gamma \frac{h^2}{2} + Ph + \tau_s dx + \gamma h S_o dx - \gamma \frac{h^2}{2} - \left(P - \frac{\partial P}{\partial x} dx \right) h \\ - \tau_b dx - 2\tau_w \left(\frac{h}{b} \right) dx = 0 \end{aligned}$$

which reduces to:

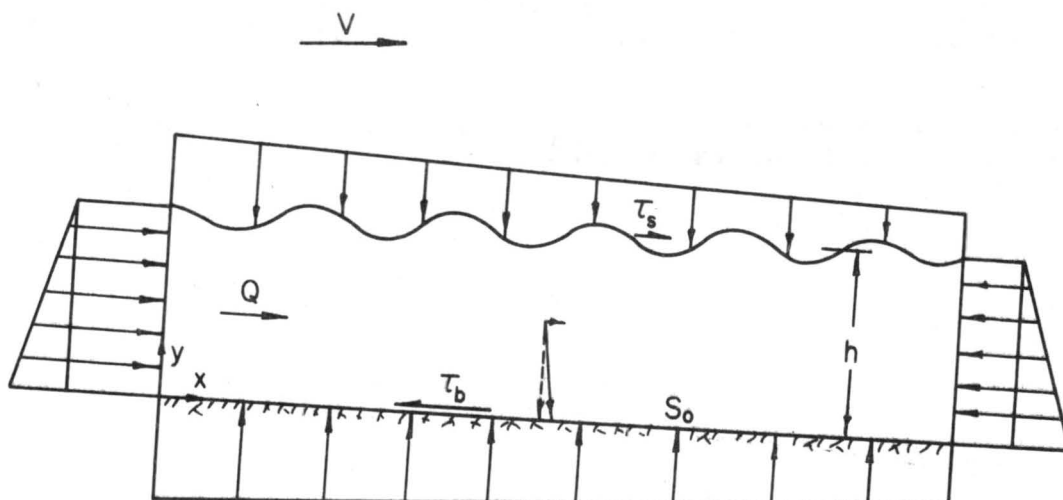


Figure 2. Forces on moving water with wind

$$\tau_b + 2\tau_w \left(\frac{h}{b}\right) - \tau_s = \tau_d = \gamma_w h \left(S_o + \frac{1}{\rho g} \frac{\partial P}{\partial x}\right) \quad (61)$$

$\tau_d = \gamma h S_c$

where τ_b is the bottom shear stress; τ_s is the water surface shear stress; τ_w denotes the shear due to the channel side walls; γ is the specific ^{weight} gravity of water; S_o is the slope of the energy gradient (slope of the channel in uniform flow); g represents gravitational acceleration; dP/dx is the air pressure gradient in the longitudinal direction, and b is the channel width. $\gamma_w = 62.4 \text{ lb/ft}^3$

For economy in writing, we shall adopt the notation

$$S_c = S_o + \frac{1}{\rho g} \frac{dP}{dx} \quad (62)$$

and

$$u_{*c} = \sqrt{\frac{\tau_d}{\rho}} = \sqrt{ghS_c} \quad (63)$$

It is worth noting that the right side of Equation (63) consists of quantities which can be measured directly.

Substituting Equation 63 into Equation (60), the expression for $\overline{\varepsilon}_y$ becomes

$$\overline{\varepsilon}_y \approx \overline{D}_y \propto u_{*c} h. \quad (64)$$

Estimation of D_T - In order to express the effective turbulent diffusion coefficient at the interface, in terms of some hydraulic parameters that would characterize the turbulent flow in the region, we assume [Monin (1959), Levich (1962), Schlichting (1965)]

$$D_T = \kappa u_{ref} l_{ref}$$

where κ is a constant of proportionality, and u_{ref} and l_{ref} are suitable velocity and length scales.

In our case we consider the surface shear velocity as a good measure of the intensity of turbulence at the surface. Also, we consider the thickness of the boundary layer, developing in the water due to the surface current, as the reference scale.

To show the development of the water boundary layer, and its variation with fetch; let us take first the case of a laterally enclosed body of water with the wind blowing along its surface. The drag exerted by the air flow first gives rise to an acceleration of the water particles near the surface. With increase in fetch, particles at deeper layers are set in motion. Then, for this enclosed body of

water, a return current is generated near the channel bottom, which is required by conservation of mass. This wind induced velocity distribution, and the variation of the resultant boundary layer, δ , with fetch is illustrated in the following diagram (from Plate, 1969).

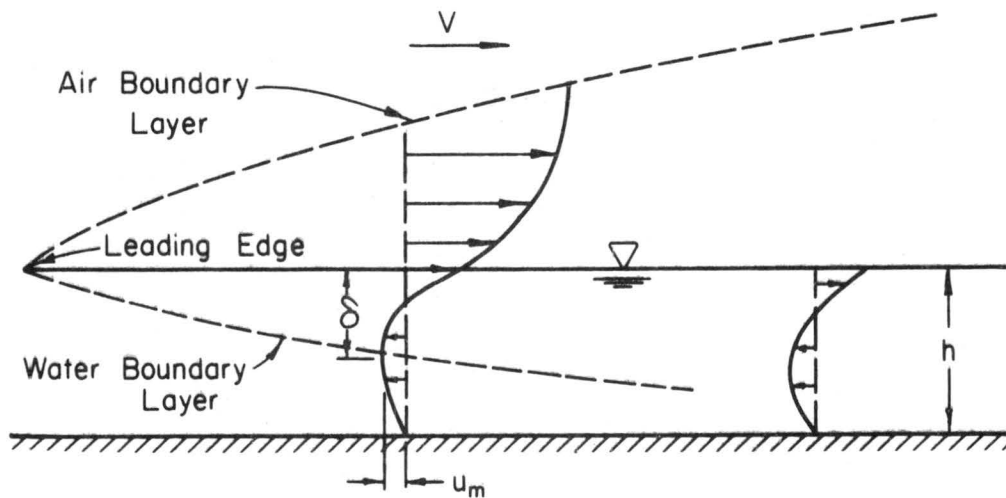


Figure 3. Distribution of wind driven currents in a standing water.

The thickness, δ , is based on the height where the current velocity $u_{(y)}$ is equal to the maximum water current velocity, u_m .

When the wind blows over the surface of a free flow of water, the velocity distribution in the water consists of the interaction of the distribution shown in Figure 3 and a logarithmic velocity distribution. For long fetches, the velocity distribution in the channel becomes independent of fetch, with the exception of small depth changes which are caused by the water surface condition. Then the

boundary layer thickness, δ , is almost constant. Consequently, for a uniform flow, the ratio of δ to h is constant. In his recent study of water surface velocities induced by wind shear, in a standing water, Plate (1969) reported that in this region $\delta \approx 0.9 h$. Thus, if we assume δ is proportional to the mean depth of flow, h , the expression for D_T becomes

$$D_T \propto u_{*s} h . \quad (65)$$

The prediction equation for reaeration with wind -
Comparing Equations (58), (64), and (65), the resultant expression is

$$k_2 = C \frac{u_{*s} h}{\nu} \frac{u_{*c}}{h} \quad (66)$$

where C is some constant of proportionality. Denoting the group $u_{*s} h / \nu$ by R_{sh} , shear Reynolds number, then

$$k_2 = C R_{sh} \frac{u_{*c}}{h} . \quad (67)$$

The above proposed formula is basically a prediction equation, and not an explanatory equation. In developing Equation (67), three separate assumptions were used. These are represented by Equations (58), (60) and (65). The development, with the assumptions used, is amenable to experimental examination. If the hypothesis used in formulating the equation is true, then C is a true constant and should not vary with the flow variations.

The surface shear velocity, u_{*s} , will be calculated from Equation (57); however, all other quantities in Equation (67) will be laboratory observed. The constant, C , will be evaluated by the statistical analysis of the observed data.

Chapter IV

EQUIPMENT AND PROCEDURES

This study was carried out in the Wind-Water Tunnel, Fluid Dynamics and Diffusion Laboratory, Colorado State University. The main objective was to determine the effect of wind on the reaeration rate constant in open channel flow. A subsidiary objective was to test the models used by the previous investigators for prediction of k_2 , with no wind blowing over the water surface.

The general procedure with and without wind, was first to set up the desired uniform flow conditions in the flume. Then the details of the flow field were measured. Individual reaeration runs were made by measuring the oxygen concentrations as a function of time at the beginning and the end of the test section. For each run, with air blowing over the water surface, the water surface displacements were recorded at six different locations in the flume.

The equipment consisted of the basic facility, the water surface gauge, a Beckman laboratory oxygen analyzer, and the device for measuring air velocity.

The Wind Tunnel Flume Combination

The flume - The laboratory flume used in this study is shown in Figure 4. It consists of truss supported channel which has a 52-ft long test section. The trusses can be rotated around a pivot by means of a screw driven support at the end of the facility.

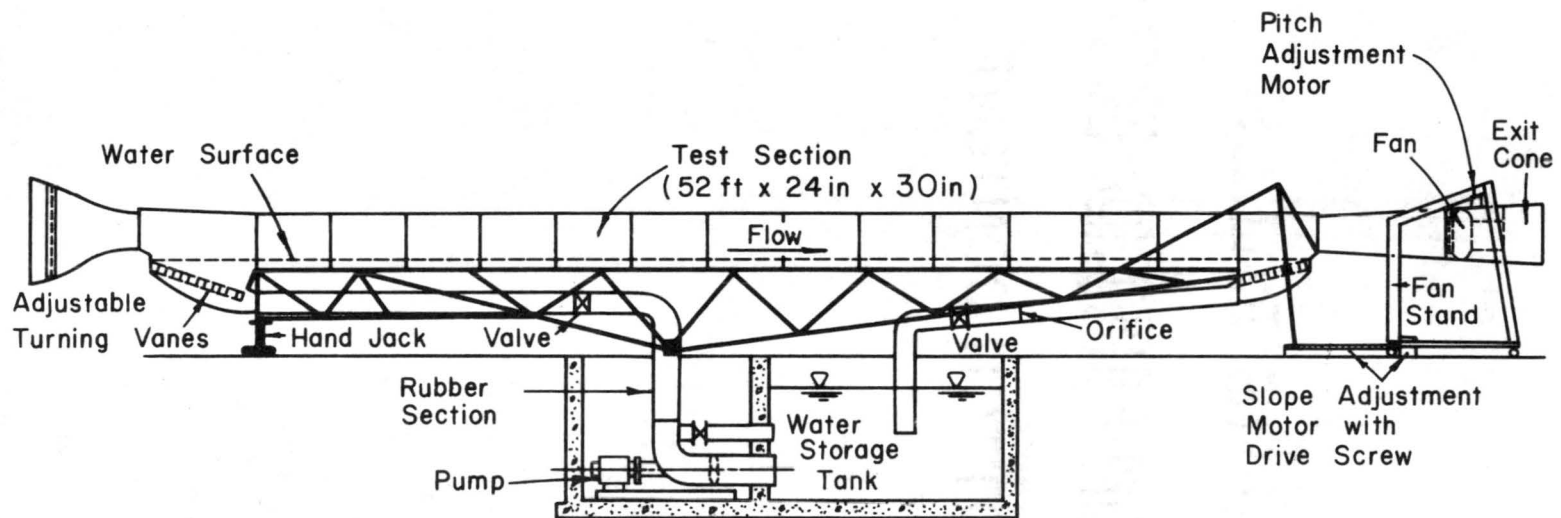


Figure 4 - Schematic Diagram of the C.S.U. Wind-Water Tunnel

Water enters the facility from the inlet section which consists of honeycomb screens. The screens serve as an effective diffuser for the incoming water, and at the same time act as wave dissipating beaches. The water flow is controlled by a pinch valve located in the supply pipe. The water leaves the test section through a honeycomb beach and returns to the sump through a metering orifice which has been calibrated in place. The pinch valve in the return pipe serves as a tailgate to control the depth of water in the test section. From the sump, the water is conveyed back into the channel by means by a three speed pump. The pump is kept at stable operating loads by means of a by-pass, controlled with a butterfly valve. At the discharge end of the pump, there is a five foot long piece of dredge hose which is capable of taking up the tilting of the system and of damping vibrations which are transmitted from the pump.

The air flow is controlled by a thirty-six inch commercial fan which is directly connected to a 15 HP induction motor. Wind speeds of 0 to 50 fps can be obtained by remotely adjusting the pitch of the fan blades. The air is taken in from the laboratory building into the entrance section. The entrance section has a bell-shaped circular inlet, two screens and a contraction cone where the air is accelerated and shaped into a jet with rectangular cross section. The contraction cone was molded in fiberglass.

Downstream from the test section the air flow is led through a honeycomb which eliminates asymmetry of the air velocity distribution. The air passes into the fan through a diffuser in which the duct cross section is changed from square to round. The air is discharged through an outlet cone into the laboratory building.

The air and water flows are both essentially three dimensional. However, in order to avoid excessive complications, we assumed a two-dimensional flow. In order to maintain the flow in the water as two-dimensional as possible, the ratio of the water depth to the channel width was kept small (to a maximum of 0.25), and the bottom of the channel was roughened. A picture of the wind-water tunnel is shown in Figure 5.

Bed roughness - Bottom roughness for the experimental channel consisted of expanded meshes, as shown in Figure 6, which were screwed to the plexiglass bottom of the channel. The observed value of the Darcy-Weisbach resistance coefficient, for the bottom roughness used, is about 0.069, for a flow depth of 0.385 ft and an average velocity of 1.02 fps.

Air Flow Measurements

A Dawyer 1/8-inch OD pitot tube was used to measure the mean air velocity. The probe was placed about 10 ft from the upstream end of the channel test section, and about 30-inch above the channel bottom. The mean air

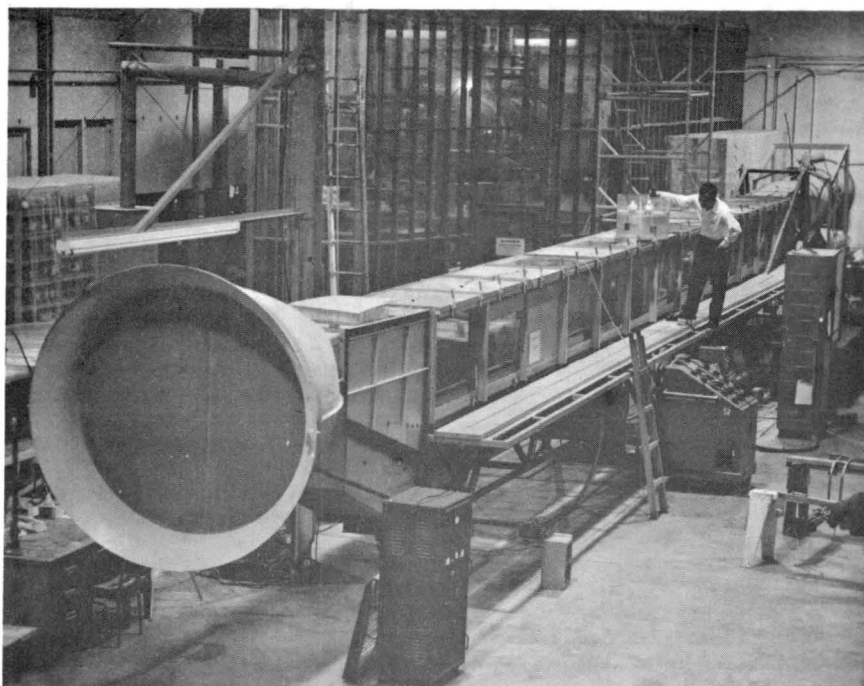


Fig. 5 - The CSU Wind-water Tunnel

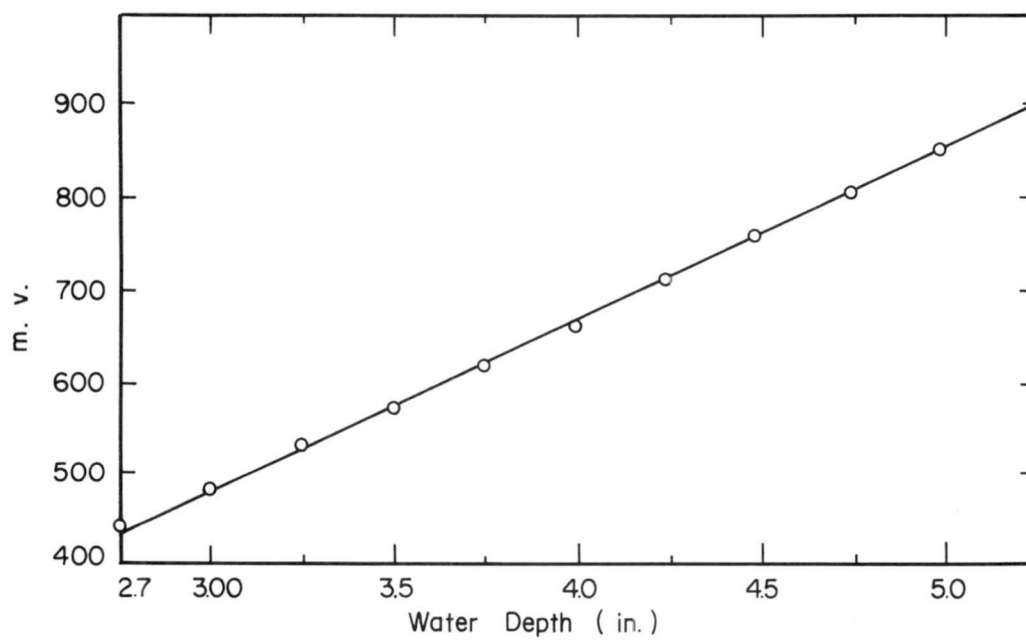
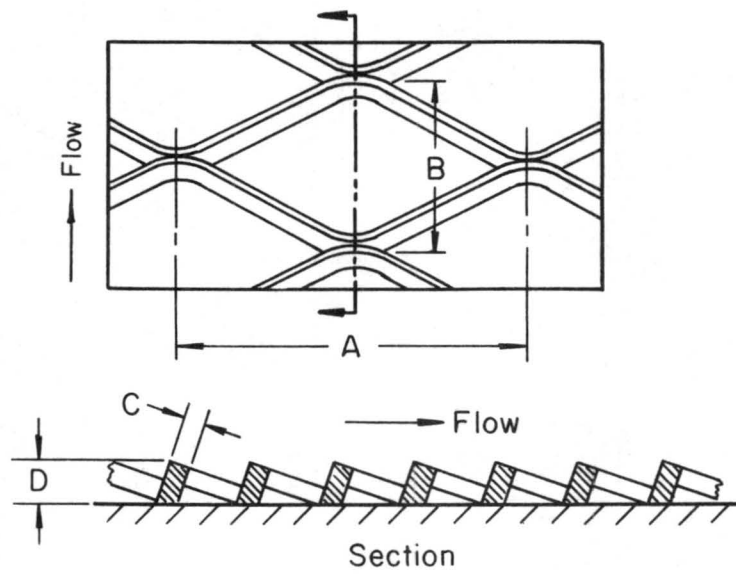


Fig. 6 - Calibration of Capacitance Wave Gauge



NOMINAL WIDTH	LENGTH A	WIDTH B	THICKNESS C	DEPTH D
1.0 "	2.00"	0.92 "	0.093"	0.197"

Fig. 7- Characteristics of Roughness Meshes

velocities measured at this location were used as reference velocities. The wind data in this study were taken at three reference velocities of 22 fps, 30 fps, and 38 fps.

To calculate the air flow, the pitot tube was connected to an electronic micromanometer, Transonic Equibar Type 120, which was calibrated against a standard water manometer.

Measurements of Water Surface Elevations

A capacitance probe with a 32-gauge nyclad insulated magnet wire was used to continuously measure the water surface displacement at a given fetch as a function of time. A sketch of this device is shown in Figure 8. The wire was stretched vertically across the flume in the center of the cross section. The water and the wire act as two "plates" of a condenser, and the wire insulation as its dielectric medium. The difference in capacitance, due to the water depth, was measured by a capacitance bridge developed in the Engineering Research Laboratory at Colorado State University. The output signal of the CSU capacitance bridge was recorded by a dual channel Brush chart recorder.

The output from the bridge was calibrated against the water depth after each series of experiments. A linear relationship between water depth and the output voltage of the capacitance bridge was obtained by changing the water depth slowly and steadily. Figure 6 illustrates this linear relationship.

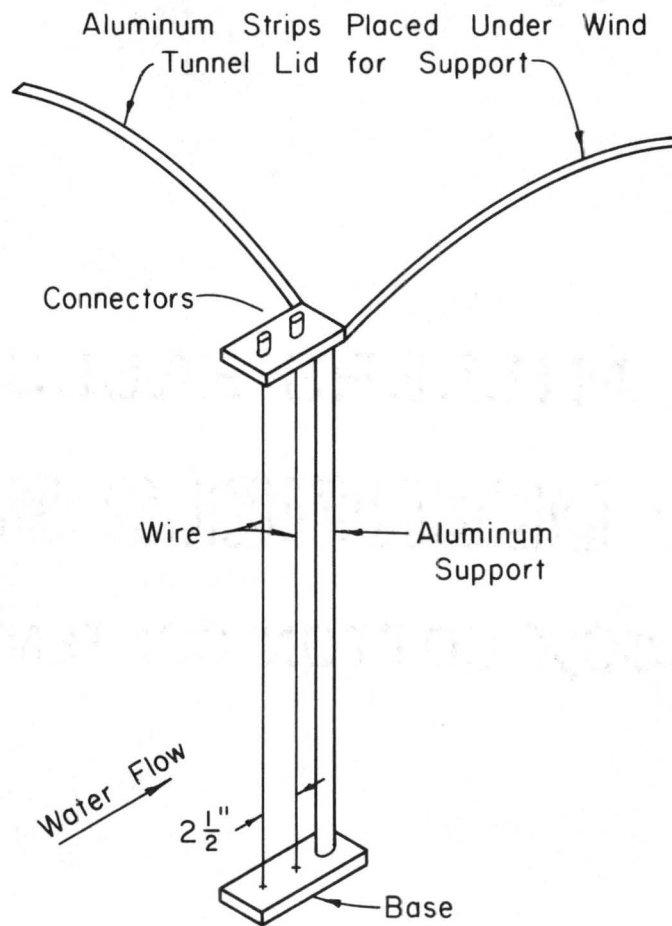


Figure 8 -Sketch of Capacitance Probe

From the wave records, the following wave properties were computed: average wave height, \bar{H} ; the average wave length, $\bar{\lambda}$; the frequency of significant waves, f , and the wave speed relative to a fixed reference system, \bar{c}_e .

Measurements of Dissolved Oxygen Concentrations

Two Beckman oxygen analyzers, model 777, were used in measuring the dissolved oxygen concentrations in the water. One instrument was located at the upstream end of the test section and the other at the downstream end of the test section.

Two basic units - a sensor and an amplifier - form the analyzer. The sensor detects the oxygen concentration, and the amplifier amplifies and attenuates the sensor signal, which may be read directly on the meter or used to drive a 0-50 mv recorder. In this study, however, the output signal was fed to a Hewlet-Packard 3440 A Digital Voltmeter and 3443 A High Gain Auto Range Unit, where a higher accuracy was attained in reading this output signal.

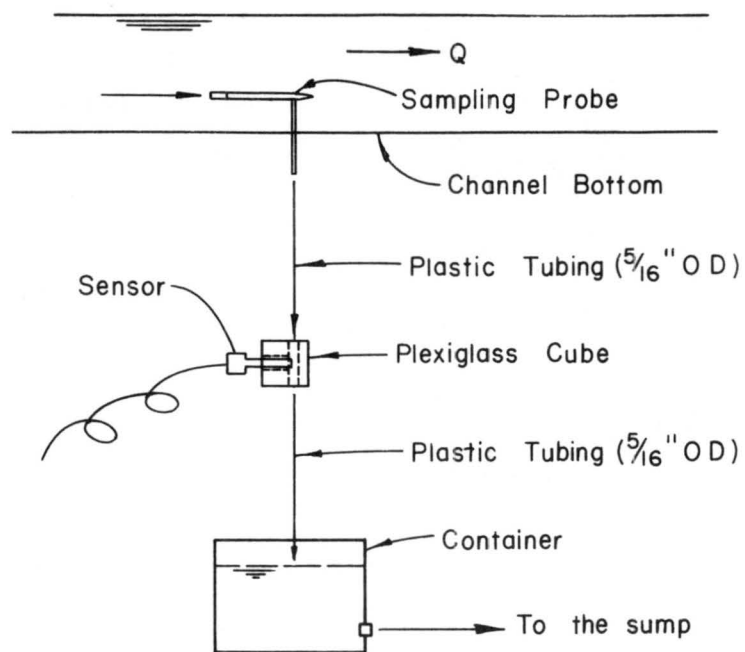
The sensor - The sensor, 2 1/2- inches long and 1/2-inches in diameter, was connected to the amplifier by a 48-inch cable. The sensor consists of a gold cathode separated by an epoxy casting from a tabular silver anode. The anode is electrically connected to the cathode by a layer of potassium chloride gel. The entire anode-cathode

assembly is separated from the sample by a gas-permeable Teflon membrane which fits firmly against the cathode surface. The inner sensor body is contained in a plastic housing and comes in contact with the sample only through the Teflon membrane. When oxygen diffuses through the membrane, it is electrically reduced at the cathode by an applied voltage of approximately 0.8 volts. This reaction causes a current to flow between the anode and cathode which is proportional to the partial pressure of oxygen in the sample.

The sensor was fitted into a 1-inch plexiglass cube so that the tip of the sensor ends at a 3/8-inch threaded hole drilled in the cube, where the water sample passes by. The sample was led from the sampling probe to the sensor through a 2-ft plastic tubing. The sensor fitting and the hydraulic circuit of the water sample is shown in Figure 9.

A sketch of the sampling probe and its arrangement in the flume is shown in Figure 10. To insure good averaging over a horizontal plane, it was designed to have a 2 1/8" x 5/16" opening, and the throat section was provided with directing vanes to draw water at a uniform rate. The connections of the sensor to the sampling probe is shown in Figure 11.

Calibration of the Beckman's oxygen analyzer - Each Beckman instrument was calibrated against the conventional



Hydraulic Circuit of the Sample Flow

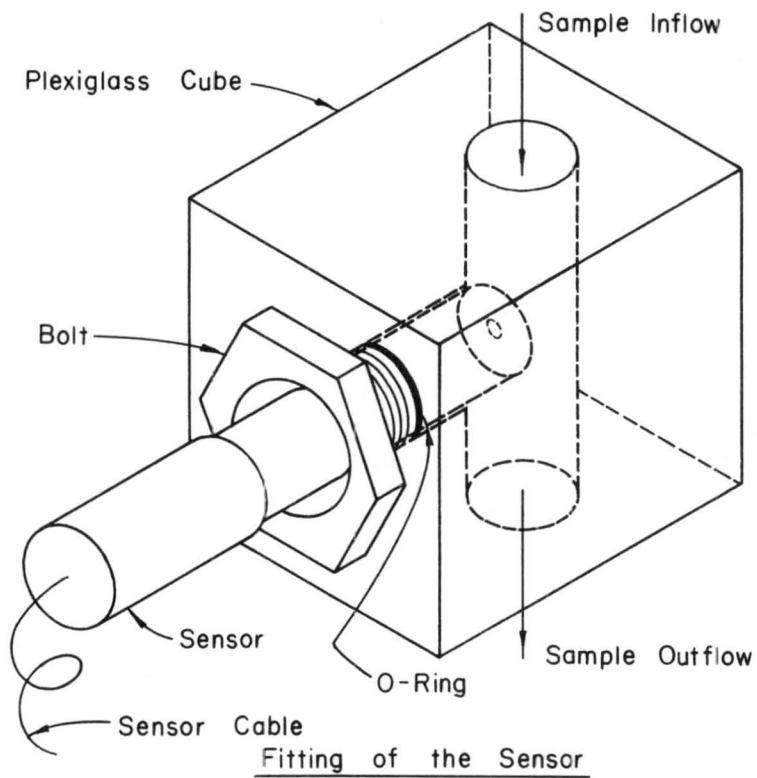
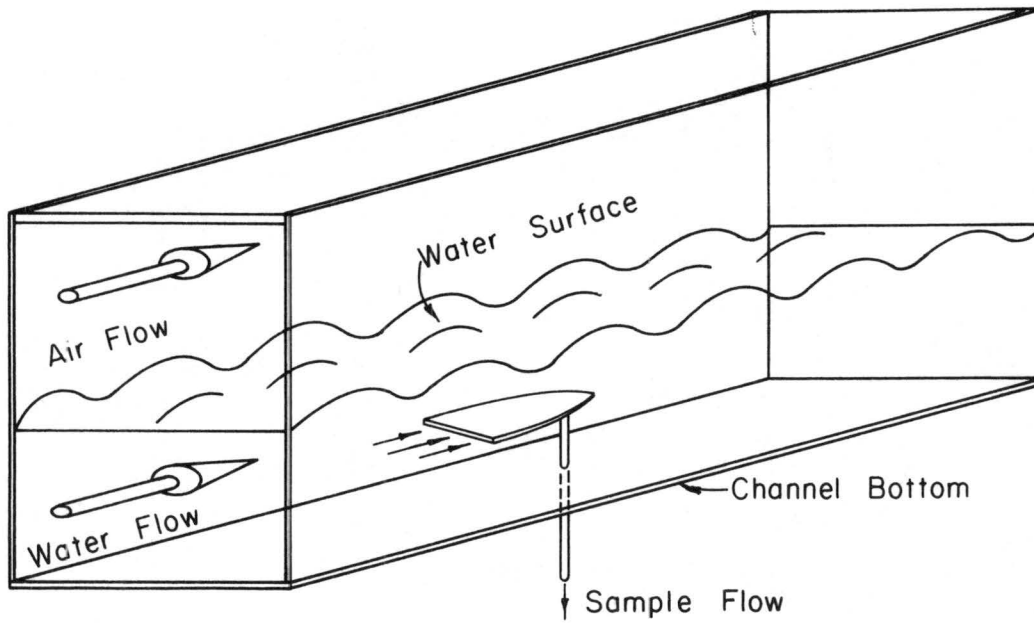
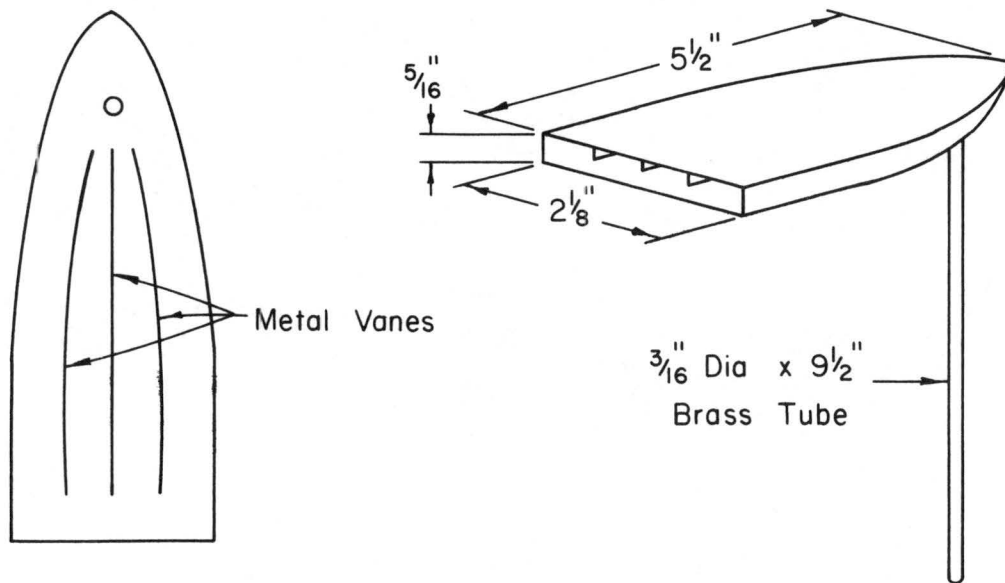


Figure 9 - Hydraulic Circuit of the Sample Flow and Fitting of the Sensor



Probe in Position



Horizontal
Section

Dimensions

Figure 10 - The Sampling Probe

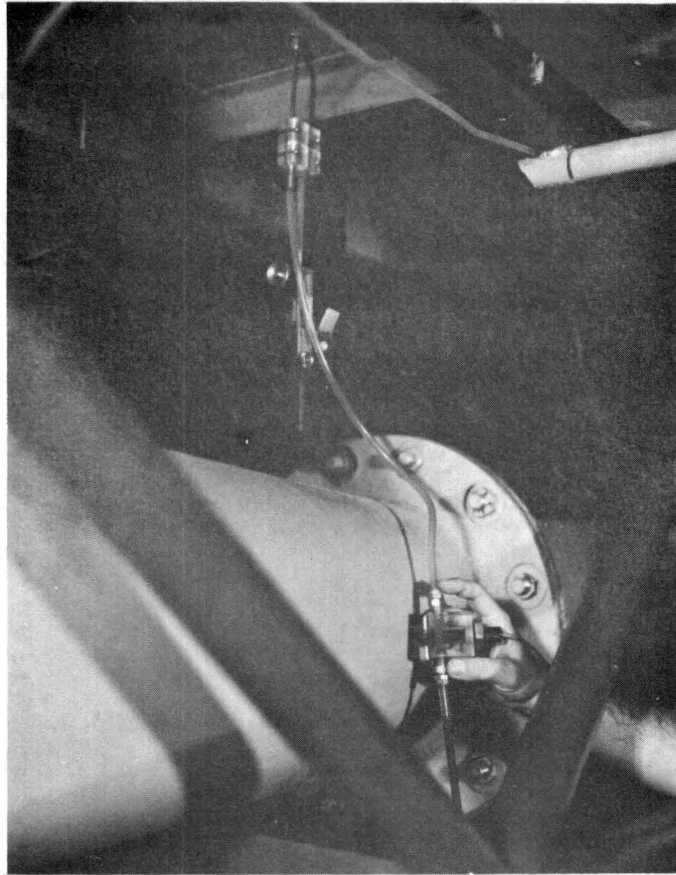


Fig. 11 -Methods of Sampling and Connections

Winkler method for analysis of dissolved oxygen; such a calibration curve is shown in Figure 12.

The general procedure used in collecting and analyzing the sample by the Winkler method was:

a. Sample was taken in 300 ml volumetric flask, by means of the sampling probe. The water was allowed to flow into the flask until two or three volumes had been displaced, after which the glass stopper was inserted.

b. The fixing reagents were added. These reagents were one pillow of manganous sulfate powder and one pillow of alkaline iodide powder.

c. The glass stopper was reinserted in a manner as to exclude all air bubbles. The bottle, then, was shaken to dissolve the powder and mix the floc that is formed. Then the floc was allowed to settle about half way down the bottle.

d. The stopper was removed and one pillow of sulfamic acid powder was added to the sample bottle. Then the mix was reshaken until the floc was dissolved; a yellow color developed if oxygen was present.

e. A 200 ml graduate was filled with the solution from the BOD bottle. This solution was then poured into a 300 ml erlenmeyer flask.

f. Using the standard PAO solution, the sample was titrated until it was pale yellow.

g. A 2 ml of starch indicator solution was added, and a blue color was formed.

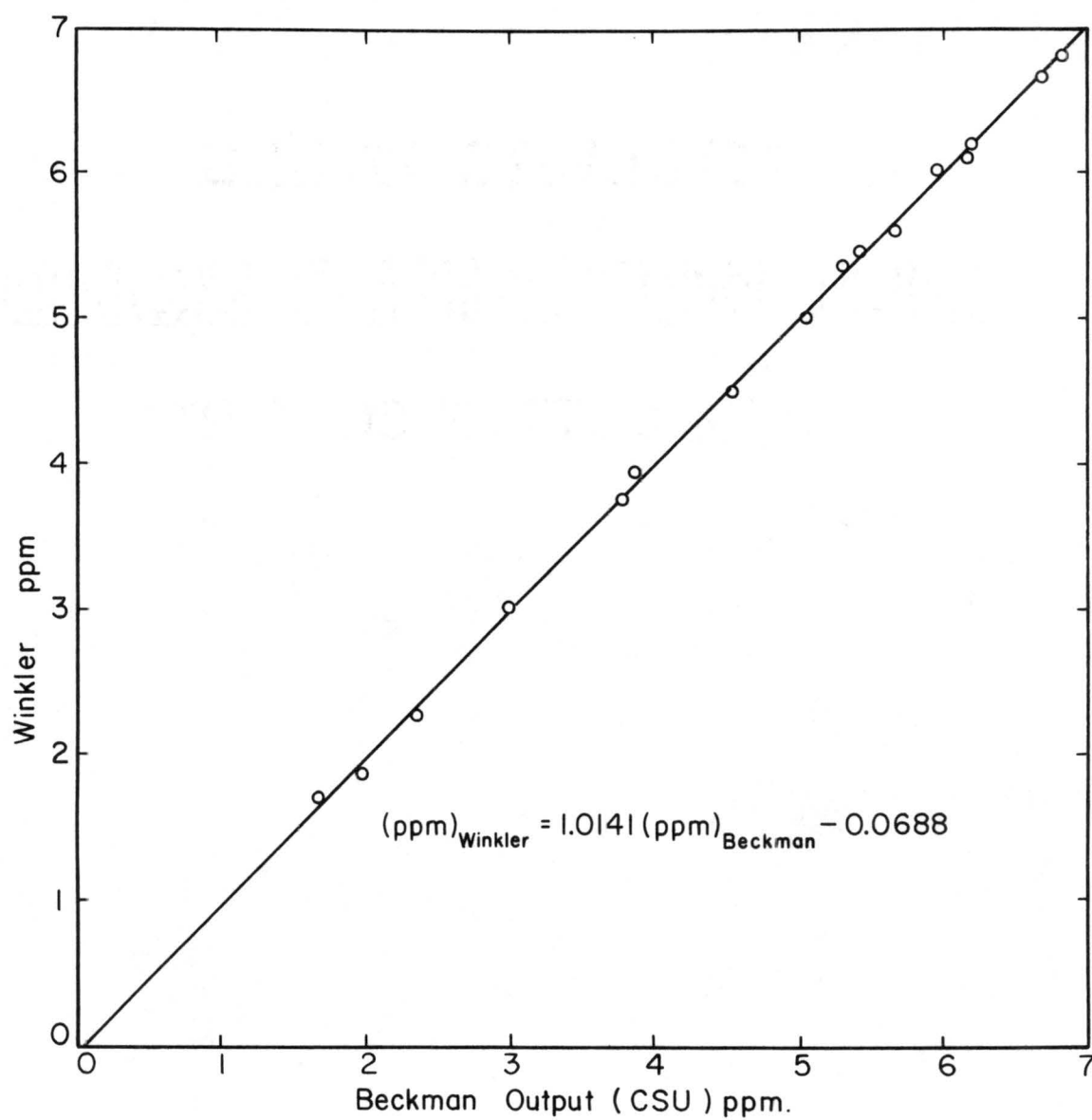


Figure 12 - Calibration of Beckman's Oxygen Analyzer

i. The titration was continued until the blue color just disappeared. The ppm dissolved oxygen is equal to the number of mls of PAO used.

When each sample was collected for analyzing by the Winkler method, the Beckman output was recorded and thus a calibration curve of the Beckman reading versus the conventional Winkler method was obtained.

Measuring Devices

The water discharge was determined by measuring the head drop across a calibrated orifice plate located in the discharge pipe. Calibration of this orifice was accomplished by removing the discharge pipe, orifice and pinch valve included, from the flume and installing the whole system in a calibration stand designed for this purpose at Colorado State University's hydraulic laboratory.

The water surface profiles, corrected for air pressure, were read from a manometer board that indicated the change in total pressure from thirteen equally spaced, 4-feet, bottom piezometer taps along the length of the flume.

The water depth was measured directly from scales attached to the side walls, with an accuracy of 0.02 inches.

The air pressure gradient was determined from pressure readings taken from thirteen taps in the top of the tunnel.

Measurement of the Reaeration Coefficient

The Adeney-Becker equation, Equation (5), implies that if the oxygen concentration at any point is continuously measured, a plot of the log of the oxygen deficit, D , versus time, results in a straight line.

The reaeration rate constant , k_2 , can be determined between any two points along the channel, separated by a time of water travel, t_o , by applying Equation (6).

Experimental procedure -- A typical procedure for measuring k_2 was as follows:

a. In order to deaerate the water in the system, a 120-liter plexiglass auxiliary tank, with two hand mixers, was used to mix the required amount of sodium sulfite with a cobalt catalyst. The stoichiometric quantity of sulfite ion required to react with the oxygen is 7.9 mg of sodium sulfite per liter per milligram of dissolved oxygen per liter. About 125 percent of the stoichiometric quantity of sodium sulfite necessary was added.

b. The chemical solution was drained into the system at the upstream end of the recirculating pump.

c. After closing the upstream pinch valve, the pump was turned on, so that the water of the flume system recirculated from the reservoir through pump and by-pass back to the reservoir.

d. When the auxiliary tank was completely drained, the upstream pinch valve was opened to allow the deaerated water to flow into the flume. Then the system was allowed to run for 15 to 20 minutes to eliminate any steep concentration gradients produced while pumping the water into the flume and to oxidize any remaining sodium sulfite.

e. The pinch valves and the butterfly valve of the by-pass were adjusted to give a uniform flow at the desired conditions.

f. After the uniform depth had been established, the Beckman oxygen analyzer was used to observe the dissolved oxygen concentration every fifteen minutes at the beginning and the end of the test section. The dissolved oxygen concentration was subtracted from the saturation value for the existing barometric pressure and water temperature during the experiment. The values of saturation oxygen, given by Churchill (1960), were used in this investigation.

Data Collection

After confirming experimentally that there was no detectable dissolved oxygen variations in the vertical direction, data was collected for runs with and without wind.

Reaeration with no air blowing-- After establishing a uniform depth for the desired conditions, the following data were recorded in each run:

a. Dissolved oxygen concentrations were measured at the entrance of the test section and at the second station downstream in the test section. Readings were taken every fifteen minutes over a period of 135 minutes.

b. Barometric pressure and the water temperature were read and recorded every fifteen minutes.

c. Water discharge was determined by measuring the head drop across the calibrated orifice plate.

d. Channel slope. The slope was determined by closing the entrance and exit pinch valves, with the pump off, and filling the test section with water. Then the water depths were measured at intervals and plotted versus distance. The slope of the best fitting line through the data equals the slope of the channel bottom. The static water surface served as a perfectly horizontal datum. For water flowing at constant depth, the channel slope was used as the slope of the energy grade line. Two channel slopes were used in this work, 0.001 and 0.00043.

e. Water depth was read from the scales attached to the sidewalks of the flume. Six uniform depths were used for each slope within the range of 1.90 to 5.73 inches.

Reaeration with the air blowing-- To establish normal depth with wind blowing and waves obscuring the average water level, an auxiliary procedure was adopted.

First, the manometer readings were taken for normal flow with no wind, to obtain the slope which must be observed on the manometer board when normal depth is reached during wind conditions. When wind was started, the resulting

action was a decrease in the normal depth, which necessitates a little increase in the discharge to raise the depth until the manometer readings were the same for normal depth with and without wind.

After establishing uniform depth for the desired condition, the following data were taken in each run.

- a. Oxygen concentrations.
- b. Barometric pressure and the water temperature.
- c. Water discharge.
- d. Channel slope. The same two channel slopes as in the case of no wind, were used.
- e. Water depth.
- f. Reference air velocity. For each channel slope, three wind velocities were used, namely: 22 fps, 30 fps and 38 fps.
- g. Air pressure gradient. This was measured for each wind velocity. A Transonics Equibar Type 120 pressure transducer was used for determining the air pressure gradients from the 13 pressure taps in the ceiling of the channel.
- h. Distance between the two sampling stations. Three distances were used, for each wind velocity, of 28-feet, 36-feet, and 44-feet. The beginning point of the test section was the same for all three lengths (4-feet from the channel inlet).

i. Wave records. Six wave records were taken for each run, at fetches of 8, 16, 24, 32, 40 and 48 feet.

Chapter V

DATA REDUCTION TECHNIQUES

The purpose of this chapter is to describe the procedure used in the reduction of the experimental data. A summary of the experiments which were performed is given first, and then the method used in computing k_2 is presented. Finally the methods used in estimating the longitudinal mixing coefficient, D_L , and the water surface shear velocity, u_{*s} , is outlined.

Summary of Experiments

Reaeration studies, made with no wind, were designated by series 1 ; those made with wind are called series 2.

In series 1, the reaeration rates were measured with the use of one distance between the reference downstream station of 44-ft.

In series 2, three distances were used of 28, 36 and 44-ft. The reference station for the measurements was held at a fixed point in the flume (4-ft. from the flume's inlet). This reference point was labeled point 1. The end points of the 28, 36 and 44- ft. distances were labeled points 2, 3 and 4 respectively. Then, section 1-2, section 1-3 and section 1-4 refer to the 28, 36 and 44-ft. distances respectively. The locations of the points in the flume are shown in Figure (13).

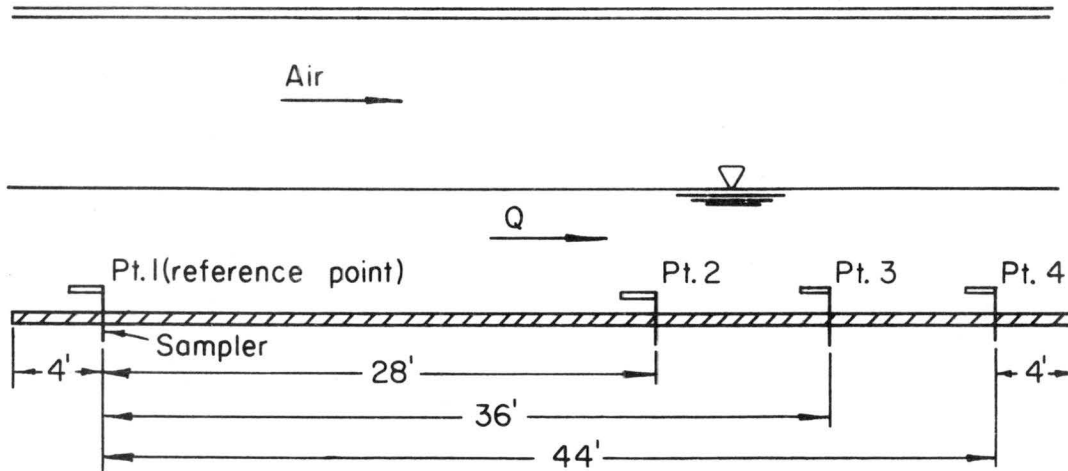


Figure (13) -- Locations of Sections in the Flume

Since the air velocity and the wave properties (height and length) varies with fetch, three short sections, where the variations of these parameters are small, were used to define local values of k_2 . These sections were : section 2-3, section 3-4 and section 2-4. The local air velocities, V_1 , in each section were computed from the measured values of the reference air velocity, V , and the air pressure gradient, by applying Bernoulli's equation. The representative value of wave height in a section was taken to be the average of the two values of " \bar{H} ", measured at the two ends of the section. To compute the k_2 values in section 2-3, for example, the following simple relationship was applied

$$8 k_2 (2-3) = 36 k_2 (1-3) - 28 k_2 (1-2)$$

where k_2 (1-3) is the observed k_2 value in test section 1-3 with length of 36 ft., at a given air velocity;
 k_2 (1-2) is the observed value of k_2 in test section 1-2 with length of 28 ft., at the same air velocity; and
 k_2 (2-3) denotes the reaeration rate constant in section 2-3 with length of 8 ft., for the same air velocity. The same technique was applied in computing the k_2 in section 3-4 and section 2-4.

Determination of k_2 for a Given Distance

For a given distance, the concentration of dissolved oxygen, at intervals of time, was observed at both ends of the section. Knowing the existing barometric pressure and water temperature, during each observation, the dissolved oxygen deficit was determined as a function of time at each end of the section. A plot of $\log D$ versus time, at the beginning of the section, on a semilog paper, results in a straight line. The same plot for the end of the section will result in a second line parallel to the first.

A least square analysis was performed, on all of the data for each experiment, to determine the best fit line. The deficit at the beginning of the section was determined from the first line, at any time " t ". The deficit at the end of the test section, at a time $t + t_0$ (t_0 is the time of flow between one end of test section to the other), was determined from the second line. Then the reaeration

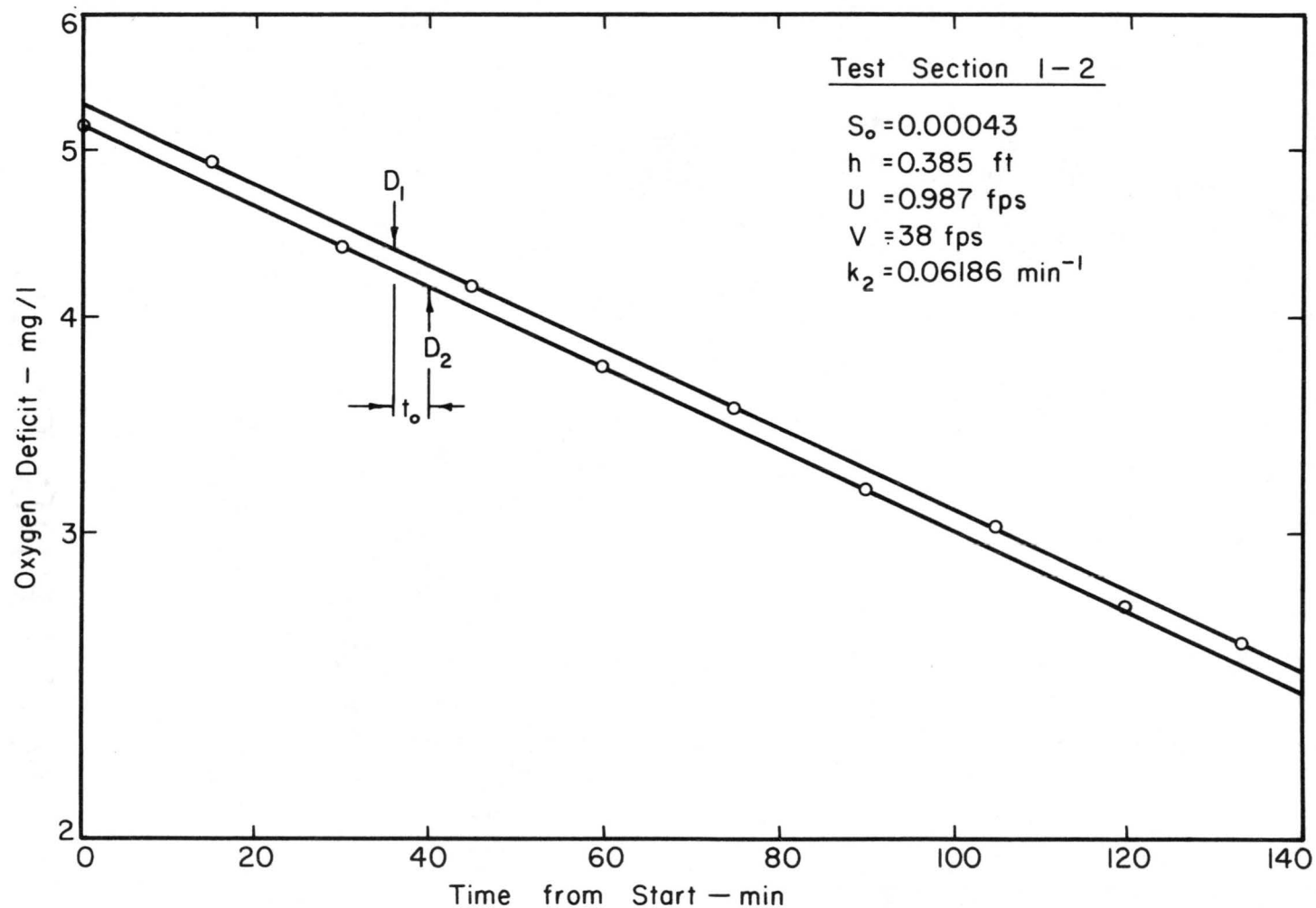


Figure 14 - Example of Reaeration Coefficient Determination

rate constant was computed by applying Equation (6). The results from a typical experiment are shown in Figure (14).

Estimation of D_L

D_L as a function of shear velocity--It has been shown in Chapter II that for two-dimensional open channel flow the longitudinal dispersion coefficient is proportional to the product of depth and the shear velocity. However, different values for the constant of proportionality have been reported. The discrepancy is partly explained by the different velocity distributions employed and by the different methods used in measuring the values of D_L .

The depth-width ratios in this experiment were about the same as in the experiment of Fischer (1967). In addition, the bed friction factor in this experiment was close to those reported by Fischer for runs with rough flume bottoms. Because of these hydraulically similar conditions, the longitudinal dispersion coefficient for this investigation was obtained by applying Fischer's empirical equations, describing D_L in a two-dimensional open channel flow with rough beds.

$$D_L = 14.6 R u_{*b} \quad (54)$$

In the above equation, u_{*b} was calculated by applying the side-wall correction given by Vanoni and Brooks (1957).

Estimation of u_{*s}

u_{*s} as a function of $V^{3/2}$ -- In this investigation, the water surface shear velocity was obtained by applying Equation (57), where

$$u_{*s} = 0.0102 V_1^{3/2} \quad \text{for } V > 6.5 \text{ ft/sec.} \quad (68)$$

In the above equation u_{*s} and the local mean stream velocity, V_1 , are given in ft/sec. This empirical formula was originally given by Hidy and Plate (1966). They derived it from a direct momentum balance relating the average slope of the water surface to the pressure gradient in the air towards the downstream direction for a well developed pattern of small wind waves.

Chapter VI

RESULTS AND DISCUSSION

This chapter begins with the presentation and examination of the results of the reaeration studies with and without wind. Then the results and discussion of the water surface properties are given. Finally, the effect of the water surface properties on reaeration are outlined.

Reaeration in Series I (Without Wind)

Reaeration as a function of velocity and depth-- A correlation analysis of the laboratory data was performed to evaluate the constants in Equation (45) , where

$$k_2 = C' U^m R^p \quad (45)$$

The preliminary analysis performed on the values of the 12 different hydraulic conditions, depths and velocities, gave $m = 1.2063$, and $p = -1.3830$.

To check the results from this investigation with those of Isaacs-Gaudy (Equation 46) and those of Churchill (Equation 47) , a second analysis of the data was performed using

$$k_2 = C \frac{U}{R^{3/2}}$$

The analysis performed on the 12 experimental results yielded the equation:

$$k_2 = 3.182 \frac{U}{R^{3/2}} \quad (69)$$

where U is in feet per second; R is in feet; and k_2 is given in day^{-1} . The correlation coefficient for the above equation was 0.869.

The constant, C , in Isaacs-Gaudy's formula is 3.283 and in Churchill's formula is 4.020. This indicates the constant determined using the field data of Churchill is higher than the constant derived from the laboratory data of Isaacs-Gandy and of this investigation.

The difference between the values of the constants, 3.182 obtained from this investigation and 4.020 obtained from the natural stream data, could be attributed to the channel geometry. In this investigation, the data was taken in a rectangular channel with uniform depths while the natural stream data was taken in irregular shaped channels. In these irregular shaped streams, the method to obtain a representative value of depths defined by the stream discharge and mean surface width, has not been firmly established. In addition, some of the field data could have been taken under a non-steady condition.

Because of the reasons mentioned above, the data of this investigation is not comparable to the field data of Churchill.

In Figure (15), values of $U/R^{3/2}$, as determined during this investigation, are shown as plotted versus the observed values of k_2 .

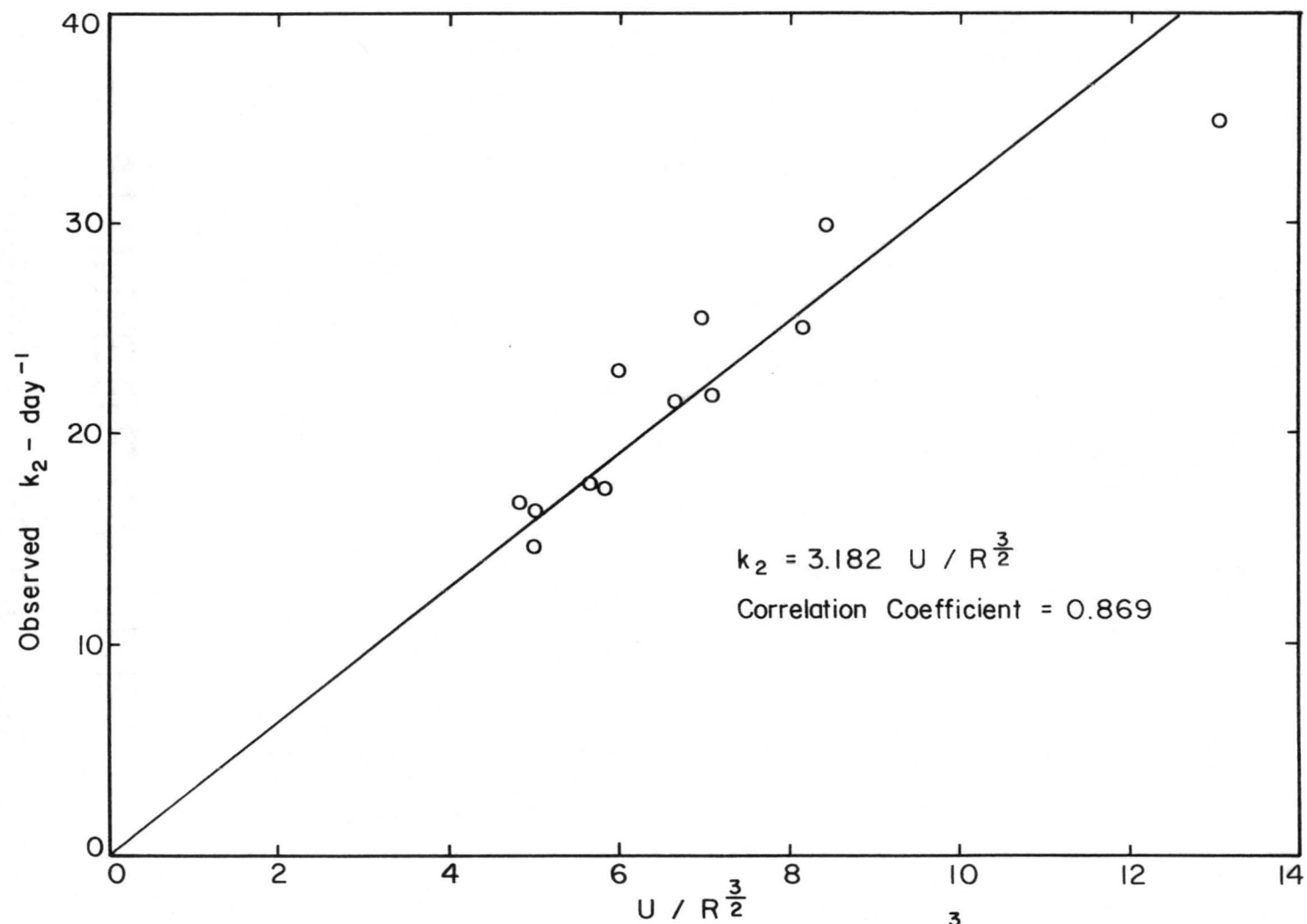


Fig. 15 - Relation of Reaeration Coefficient to $U/R^{\frac{3}{2}}$.

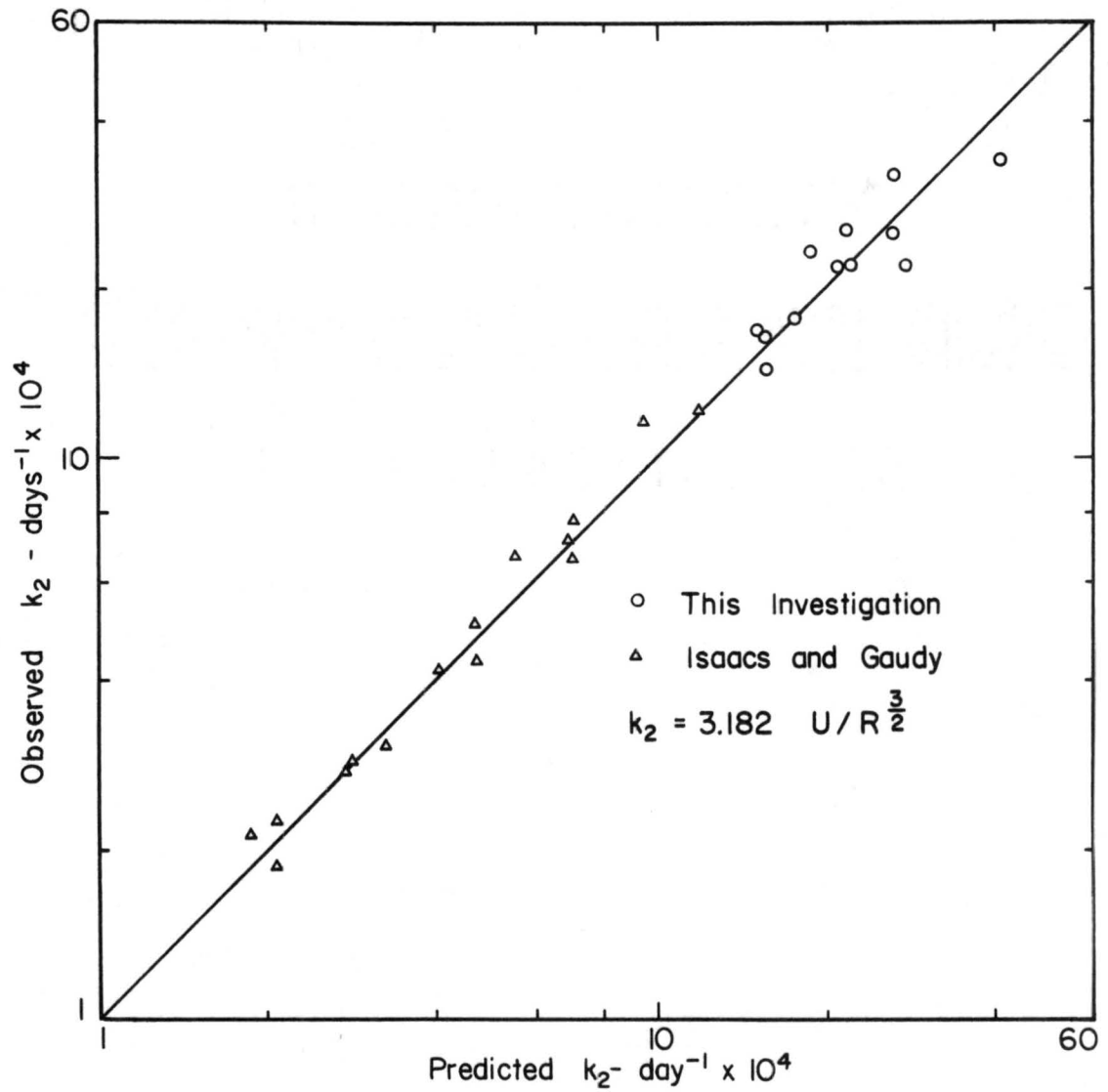


Fig.16 - Observed versus Predicted Values of k_2 .

Figure (16) shows a comparison of observed k_2 and computed k_2 , from Equation (69), using the data of this investigation and data reported by Isaacs-Gandy. The figure indicates that both data fit the predicting equation. The values calculated from the equation are referred to as the "predicted" coefficients; those computed from oxygen data, as the "observed" coefficients.

Reaeration as a function of D_L -- Krenkel (1960)
 was the first to show that the reaeration coefficient, k_2 , may be related to the longitudinal dispersion coefficient, D_L . The fundamental equation was assumed to have the form

$$k_2 = C D_L / R^2$$

where he considered D_L as a measure of the frequency of collision of gas molecules with surface water layers.

The analysis on the data from this experiment yielded the following predictive equation

$$k_2 = 0.000053 \frac{D_L}{R^2} \quad (70)$$

Comparing Equations 41, 42, and 70, we note that the k_2 values of this investigation and of Krenkel are about 3.5 times those of Thackston. Krenkel and Thackston noted the 3.5-fold difference in the constants, where

Thackston stated that after checking over Krenkel's data, no mistakes in procedures or mathematics were discovered, and that no explanation for the apparent differences could be found.

It is worth noting that the channel width used in this investigation, 2-feet, is the same as that of Thackston, but it is twice the width used by Krenkel. However, the depth-width ratios used in this investigation are several times larger than those reported by both investigators. It is not clear why Thackston's data and those of both Krenkel's and this investigation are significantly different.

In Figure (17), values of D_L / R^2 as determined during this investigation are shown plotted versus the observed values of k_2 . The high correlation coefficient, which is 0.955, lends weight to the general validity of Equation (70).

Figure (18) shows a comparison of observed k_2 and predicted k_2 , from Equation (70), using the data of this investigation and the data reported by Krenkel.

Reaeration as a function of shear velocity-- Thackston formulated the following expression for k_2 , in relation with u_* :

$$k_2 = C \frac{u_*}{h} \quad (35)$$

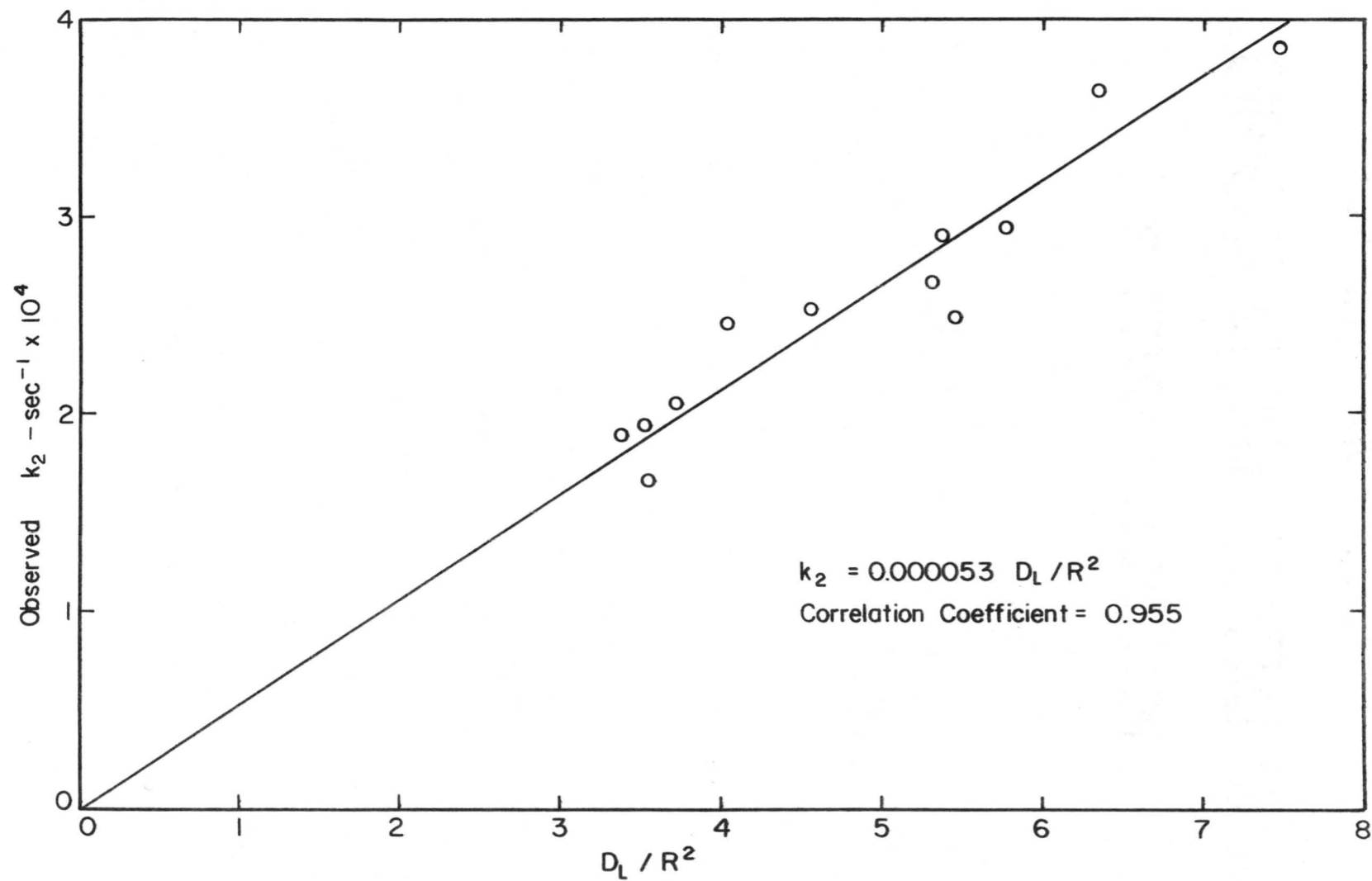


Fig. 17 - Relation of Reaeration Coefficient to D_L / R^2

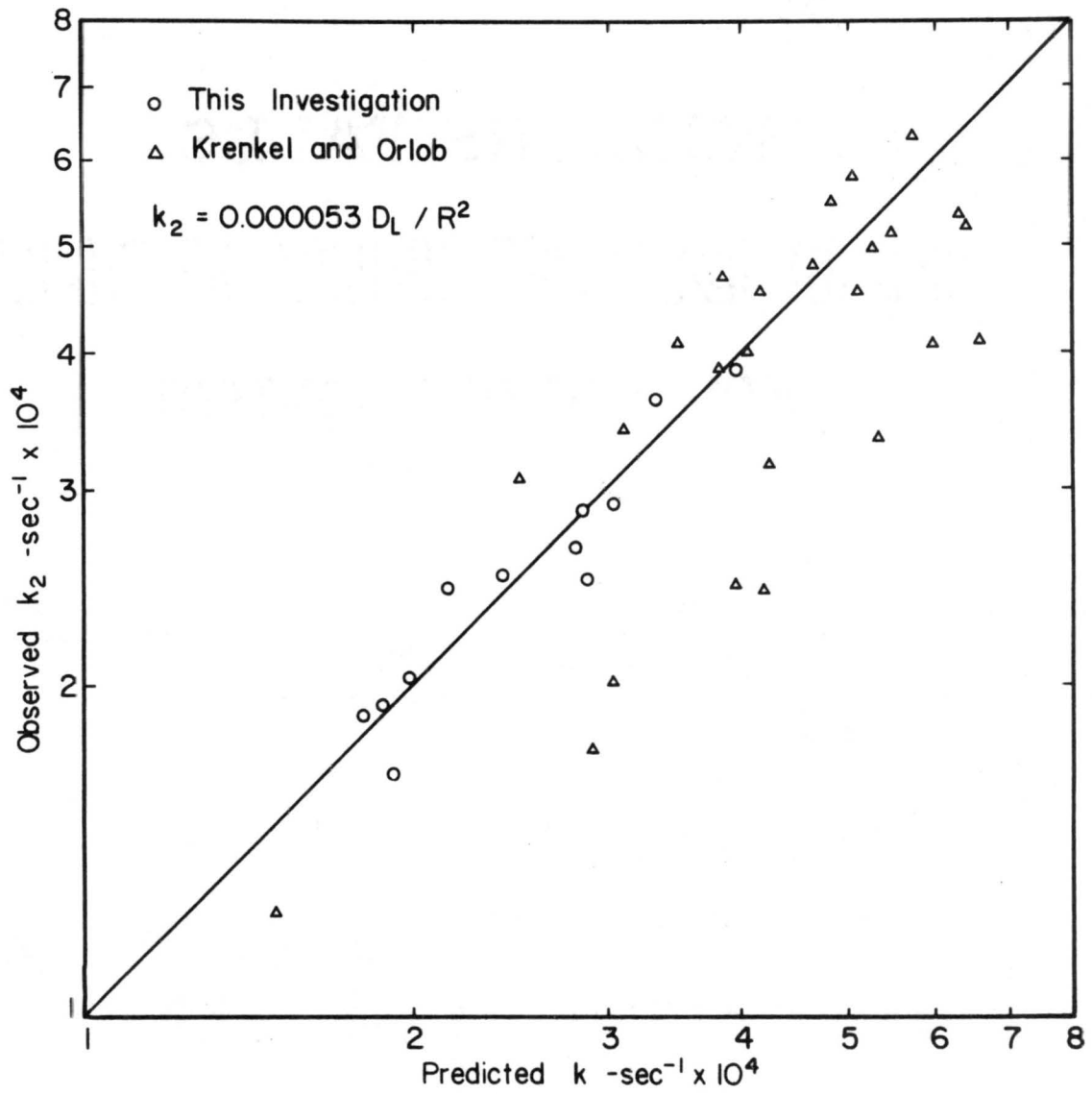


Fig. 18 - Observed versus Predicted Values of k_2 .

When the above equation was tested by correlation analysis of the laboratory data, from this investigation, the following equation was obtained:

$$k_2 = 0.000776 \frac{u_{*b}}{R} \quad (71)$$

in which u_{*b} is the water shear velocity calculated by applying the side-wall correction procedure of Vanoni and Brooks (1957). We adopted this method, in determining u_* , because of the relatively large depth-width ratios used in this investigation and because of the roughened channel bed employed in the experiments. It should be noted here that a hydraulic radius corrected due to the side wall effect, R_b , should be used instead of R . However, to be consistent with the parameters used by earlier investigators, the hydraulic radius R was adopted in the correlation analysis. The systematic error induced by using R instead of R_b , was calculated to be within the range of 8% to 20%, depending on depth of flow.

The k_2 values of this investigation are larger than those reported by Thackston by a factor of about 3.6. This discrepancy is illustrated in Figure (19). It can be seen that the predicted values, using Equation (71) are lower than the observed values of Thackston. As already mentioned, no explanation for the apparent differences could be found. It is only apparent that a recheck of Thackston's laboratory investigation is needed, with a hope that the results will lead to a fundamental

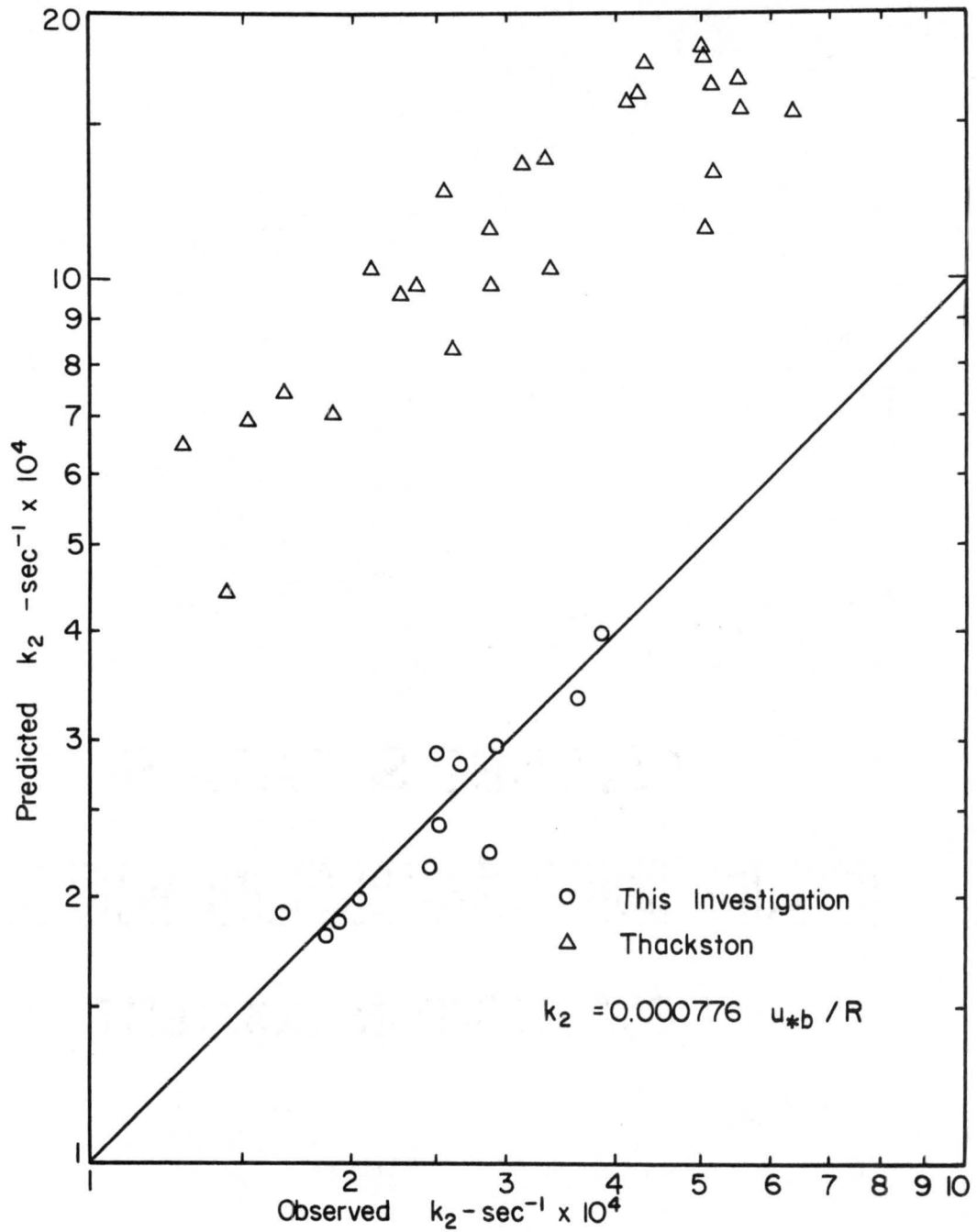


Fig. 19 - Observed versus Predicted Values of k_2 .

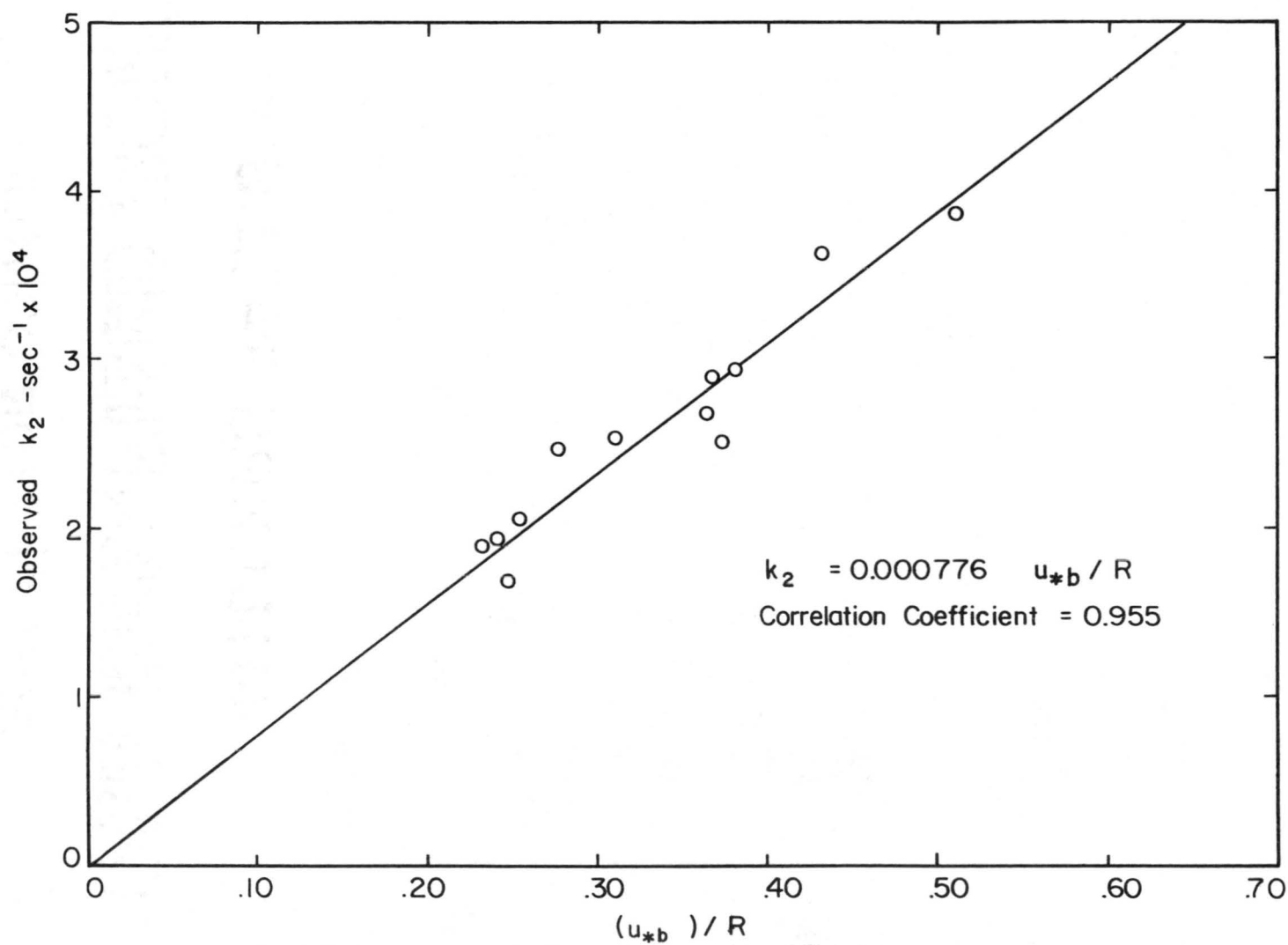


Fig.20-Relation of Reaeration Coefficient to u_{*b} / R .

understanding of the functional relationship between k_2 and the hydraulic parameters.

In Figure (20), values of u_{*b}/R as determined during this investigation were shown plotted against the observed values of k_2 with a correlation coefficient of 0.955.

Characteristics of the prediction equations-- In Equation (69) , the reaeration rate constant was expressed in terms of the two basic variables, U and R . These two variables are independent of each other and, therefore, neither the exponent of R nor of U is influenced by the inclusion of the other hydraulic parameters in the multiple regression analysis, such as the channel slope S_o .

In Equations (70) and (71) both D_L and u_{*b} are strongly dependent on R . None of the exponents of these variables can be relied on to give a true indication of the effect of the corresponding variables on k_2 . In addition, and as previously mentioned, that for a uniform two-dimensional flow with no lateral velocity profile, the longitudinal dispersion coefficient is directly related to the shear velocity, u_{*b} , and the depth, h , as illustrated in Equation (54). Consequently, Equations (70) and (71) differ by a constant factor only. Both equations are valid prediction equations, though they offer no advantages over prediction Equation (69).

Reaeration in Series II

Reaeration as a function of u_{*s} and u_{*c} -- In chapter III a functional relationship between k_2 , u_{*s} and u_{*c} was derived, Equation (67), to define the reaeration rate with wind blowing along the water surface. To test this functional relationship against the laboratory data, the fundamental equation was assumed to have the form

$$k_2 = C' \left(R_{sh} \right)^p \left(\frac{u_{*c}}{h} \right)^q \quad (72)$$

in which C' , p and q are constants.

A multiple correlation analysis was performed on the tabulated experimental data to determine the value of the constants. This analysis produced the equation

$$k_2 = (2.66 \times 10^{-8}) R_{sh}^{1.0414} \left(\frac{u_{*c}}{h} \right)^{1.0583} \quad (73)$$

for which the multiple correlation coefficient was 0.9943.

The rather high degree of correlation between the variables and the fact that p and q values are close to 1.0, as was suggested by previous theoretical considerations, gives support to a theoretical form of the relationship

$$k_2 = C R_{sh} \frac{u_{*c}}{h} \quad (67)$$

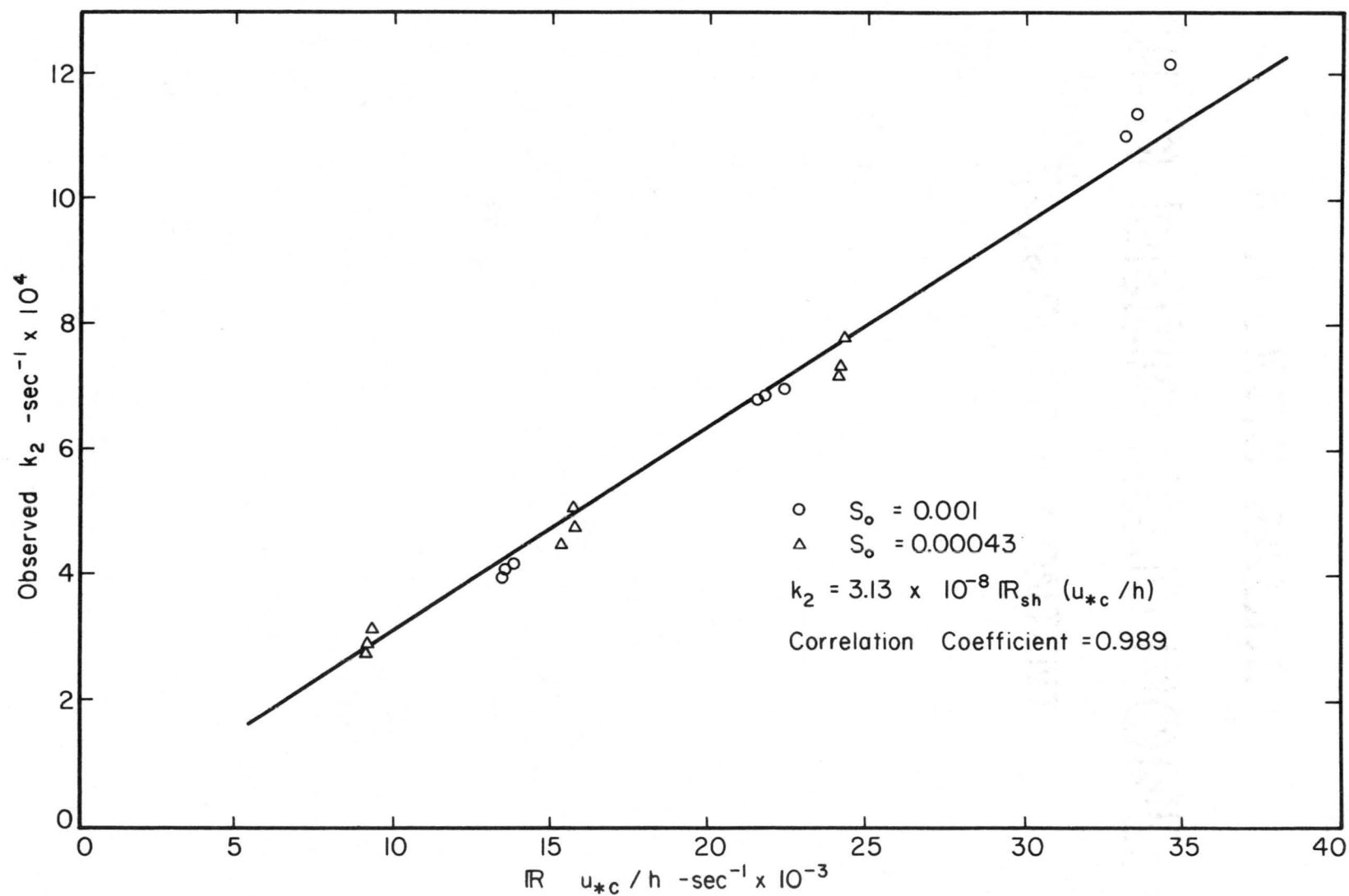


Fig. 21 - Relation of Reaeration Coefficient to $IR_{sh} (u_{*c} / h)$

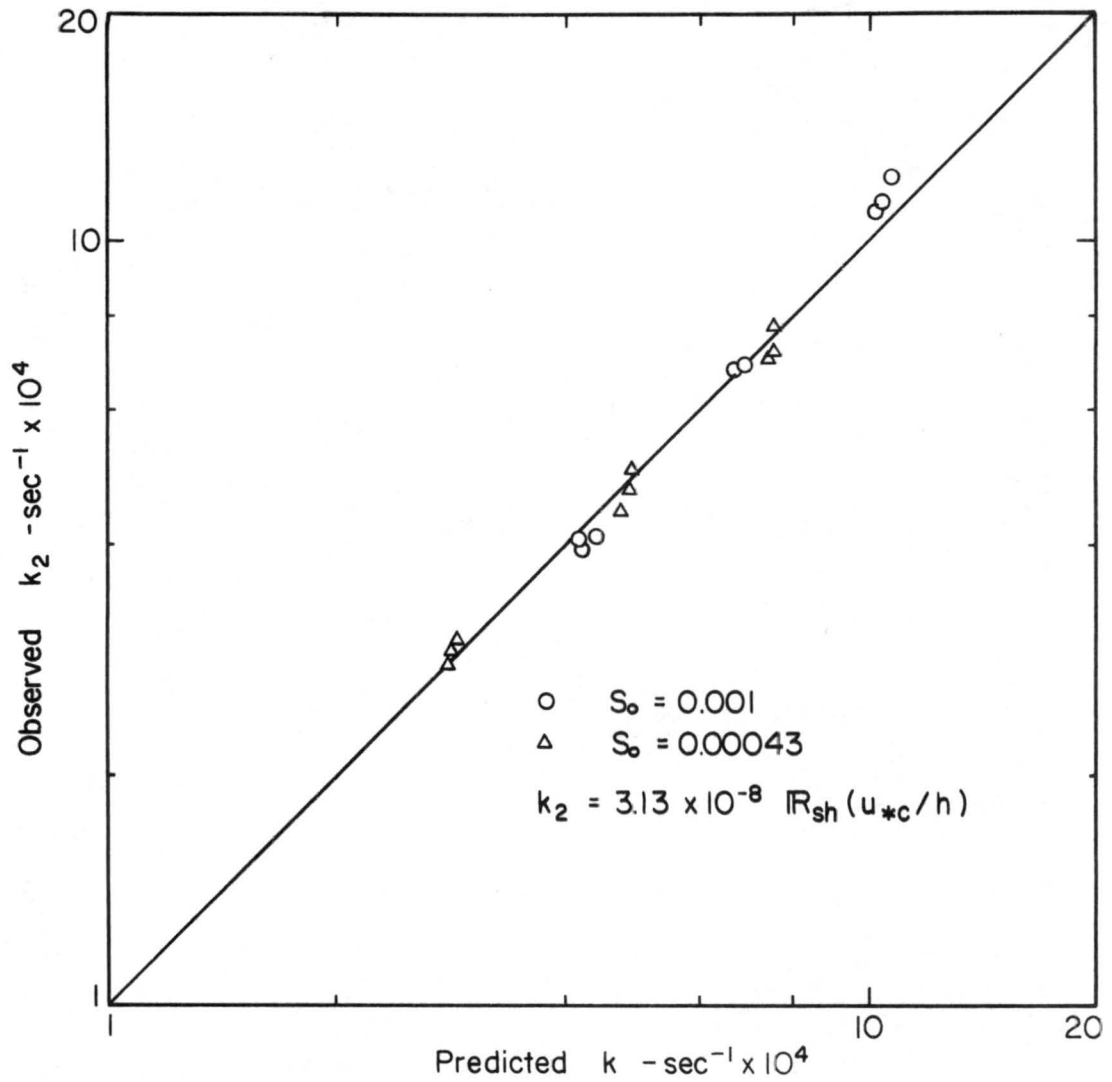


Fig. 22 - Observed versus Predicted Value of k_2 .

A second analysis of the data was performed using Equation (67). The analysis yielded the predictive equation

$$k_2 = (3.13 \times 10^{-8}) R_{sh} \frac{u_{*c}}{h} \quad (74)$$

where k_2 is given in sec^{-1} ; u_* is ft/sec., and h is in ft. in which the correlation coefficient was 0.989. Figure (22) shows the observed data in relation to the computed regression line. The constant in Equation (74) is a general dimensionless constant of proportionality.

Advantages of the developed equation-- The ultimate objective of this investigation was to develop a practical method to predict the rate of reaeration in natural streams and rivers with wind blowing over the water surface, using easily obtainable hydraulic parameters. Referring to Equations (63) and (68), it can be deduced that Equation (74) is based only on the independent variables... V , h , $\frac{dp}{dx}$ and S_o . All these parameters, except, perhaps, the parameter $\frac{dp}{dx}$ are some of the simplest hydraulic variables to measure. In the field, however, one can ignore $\frac{dp}{dx}$.

The high degree of correlation between the variables, and the fact that p and q , in Equation (72), are close to their theoretical value, lends weight to the general validity of Equation (74) throughout the range of data.

Applications of the equation--Equation (74) was developed under the conditions of two-dimensional uniform flow. The constant was evaluated using laboratory data taken under ideal conditions, where neither synthetic detergents, containing anionic surface-active agents, nor sources or sinks of oxygen were present.

Equation (74) should be applied only to reaches with uniform flow, where the hydraulic variables are considered constant.

In applying Equation (74) it should also be realized that surface active agents, such as detergents, may greatly affect the results. The percentage reduction in the rate of aeration attributable to the surface active detergents depends on both the initial value of the oxygen absorption rate and on the concentration of surface active agent. Gamson et. al. (1955) reported as much as a 50% reduction in k_2 for a concentration of two parts of active matter per million parts of water. A corresponding correction factor must therefore be applied after the basic value of k_2 has been calculated from Equation (74).

Equation (74) should also not be applied to stream reaches where a significant quantity of "white water" exists, where entrainment of air bubbles results in a greater rate of reaeration than that predicted by the proposed equation.

The absolute lower limit for the range of application of the formula is that of $V = 6.5$ fps, below which the predictive equation for u_{*s} , Equation (68), is not applicable (Plate and Hidy (1967)). The upper limit is when the air flow is so intense that the waves start breaking. The condition of breaking waves is not included in the model used in developing the proposed formula. It will cause the rate of reaeration to substantially exceed the rate predicted by the proposed equation. This increase is partly due to the increase of rate of surface renewal, i.e. as the crests of the waves break off, a new layer of water is exposed to the air, and is instantaneously saturated with oxygen, leading to an increase in the rate of reaeration. Furthermore, as the waves break, the mass of fluid from the crest of the waves disintegrates into spray which gets saturated before it drops and mixes with other masses of fluid onto the surface. The result is an increase in mixing, due to the spray impact, and a higher oxygen concentration directly due to the droplets' high oxygen concentration.

The constant in the developed equation was based on observations with neutrally stratified flow; thus the equation should be applied to reaches in which no vertical stratification exists.

Properties of the Water Surface

The condition of the water surface should be an important factor affecting the rate of reaeration. The properties of the surface waves, determined for this investigation, are given in Table (3). The symbols have been described in the list of symbols with the units which were used to describe the parameters.

The growth with fetch of waves in the channels is reflected in two characteristic lengths, the average wave height, \bar{H} , and the average wave length $\bar{\lambda}$. The variations with fetch and wind speed of \bar{H} and $\bar{\lambda}$ are shown in Figures (23) and (24), respectively.

It appears from Figure (23) that there is an initial linear growth of waves with distance, followed by an exponential increase and a "leveling off" of growth levels for the large fetches. However, at the low wind speed, the calculated waves amplitude shows little deviation from the linear rate of growth. The results demonstrate that on a qualitative basis the rates of growth of wind generated waves are compatible with the theoretical proposals of Phillips (1957) and Miles (1957), which predict an initial linear growth followed by an exponential increase. A "leveling off" in the wave growth will be attained when the rate at which energy is transmitted from the air to the waves is balanced by the rate of viscous dissipation in the liquid. The dissipation of energy in small gravity-

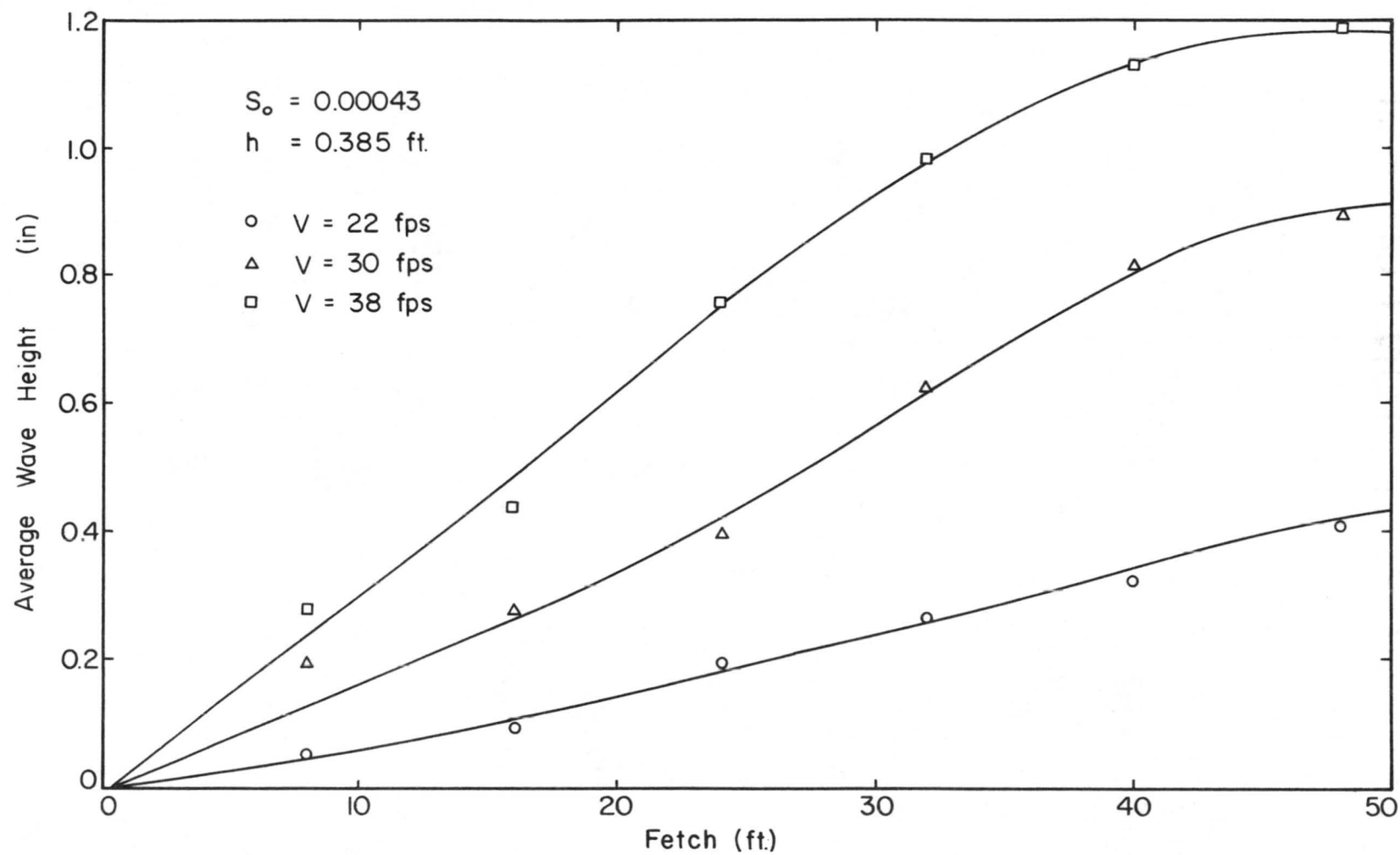


Fig. 23 – Variation of the Average Wave Height with Fetch and Air Velocity.

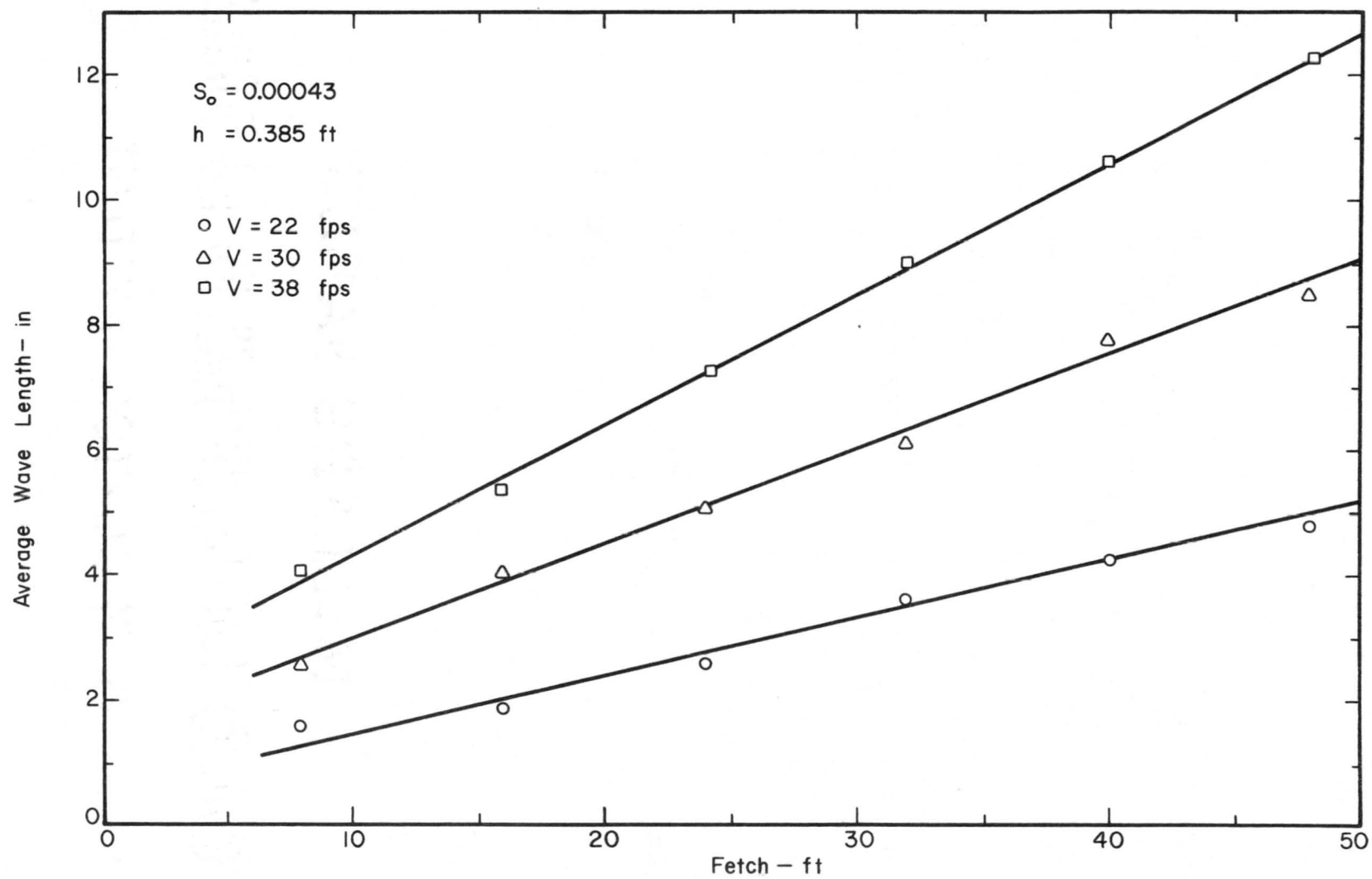


Figure 24 - Variation of the Average Wave Length with Fetch and Air Velocity

capillary waves is probably related to the action of viscosity and surface tension. The loss by viscous forces is proportional to $(ak)^2$ (Lamb (1932)), where a is the wave height and k is the wave number. Longuet-Higgins (1962) proposed a theory for the transfer of energy from gravity waves to capillary waves. As a gravity wave reaches its maximum steepness, surface tension effects become important as a sharp crest develops. These effects result in the generation of capillary waves at or near the gravity-wave crests. Longuet-Higgins calculated the steepness of the capillary waves and also estimated the dissipation of energy by the capillary waves. The energy dissipated by a capillary wave with height a_c and wave number k_c was found to be proportional to $(a_c^2 k_c^3)$. A leveling out in the growth rate of waves will occur, when the action of these dissipative processes is balanced by the input of energy from the air motion.

Another phenomenon common to all the results observed is the decrease of the average frequency of the significant waves, as distance along the flume increases. Figure (25) shows the variation of "f" with fetch and V . The tendency for the frequency to assume a constant value--as suggested by the leveling out of slopes of the curves--must be expected as the growth of the lower frequency waves becomes restricted by the limited water depth used in the experiment.

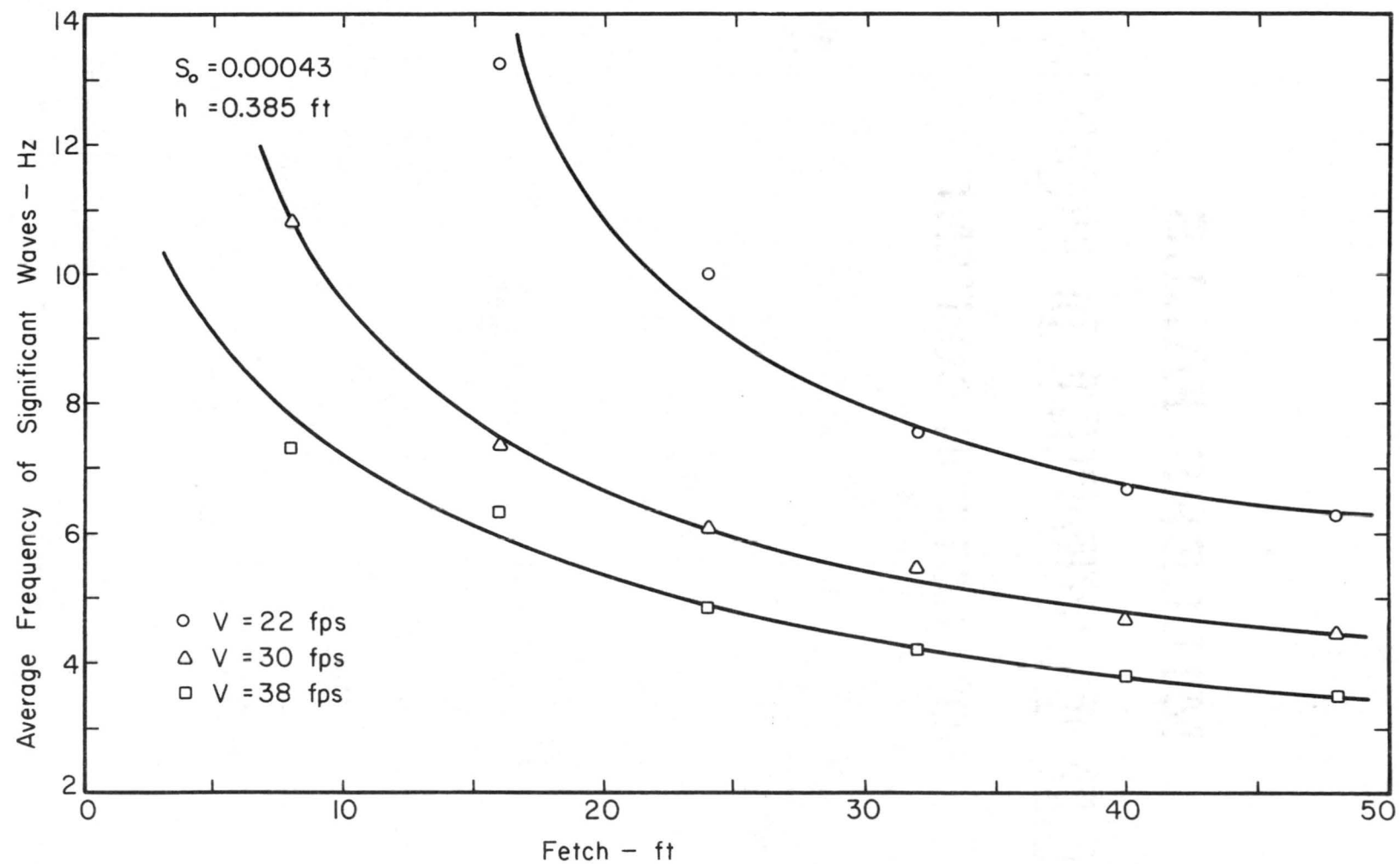


Figure 25—Variation of the Average Frequency with Fetch and Air Velocity

Presumably, on deeper water, the frequency would continue to decrease as longer waves are generated.

To account for the effect of the wave height, \bar{H} , on the surface shear velocity, the variation of \bar{H} and u_{*s} with fetch are shown in Figure 26, and the effect of u_{*s} on \bar{H} and f at a fixed position, is shown in Figure 27. There exist some coupling between \bar{H} and u_{*s} , that is, the initial wavelets are generated and developed by the shearing stress and the shearing stress is in turn increased by the generation and development of initial wavelets. The increase of u_{*s} with fetch is shown to be approximately linear. The change of \bar{H} and f was comparatively large when the values of u_{*s} were small.

With independent measurements of the water mean velocity, U , the average wave length, $\bar{\lambda}$, it is possible to determine if the mean wave speed relative to a fixed reference system is greatly different from the theoretical. The classical wave celerity for small amplitude gravity waves, accounting for a mean velocity in the water, is, for finite depth h , given by (Kinsman (1965))

$$c_t = \frac{g}{k} \tanh kh + \frac{k\sigma}{\rho} \quad (75)$$

onto which the mean water velocity must be superimposed. In the above equation: h is the depth of water; σ and ρ denote the surface tension and density of the water, respectively, and $k = 2\pi/\bar{\lambda}$ is the wave number. Possible

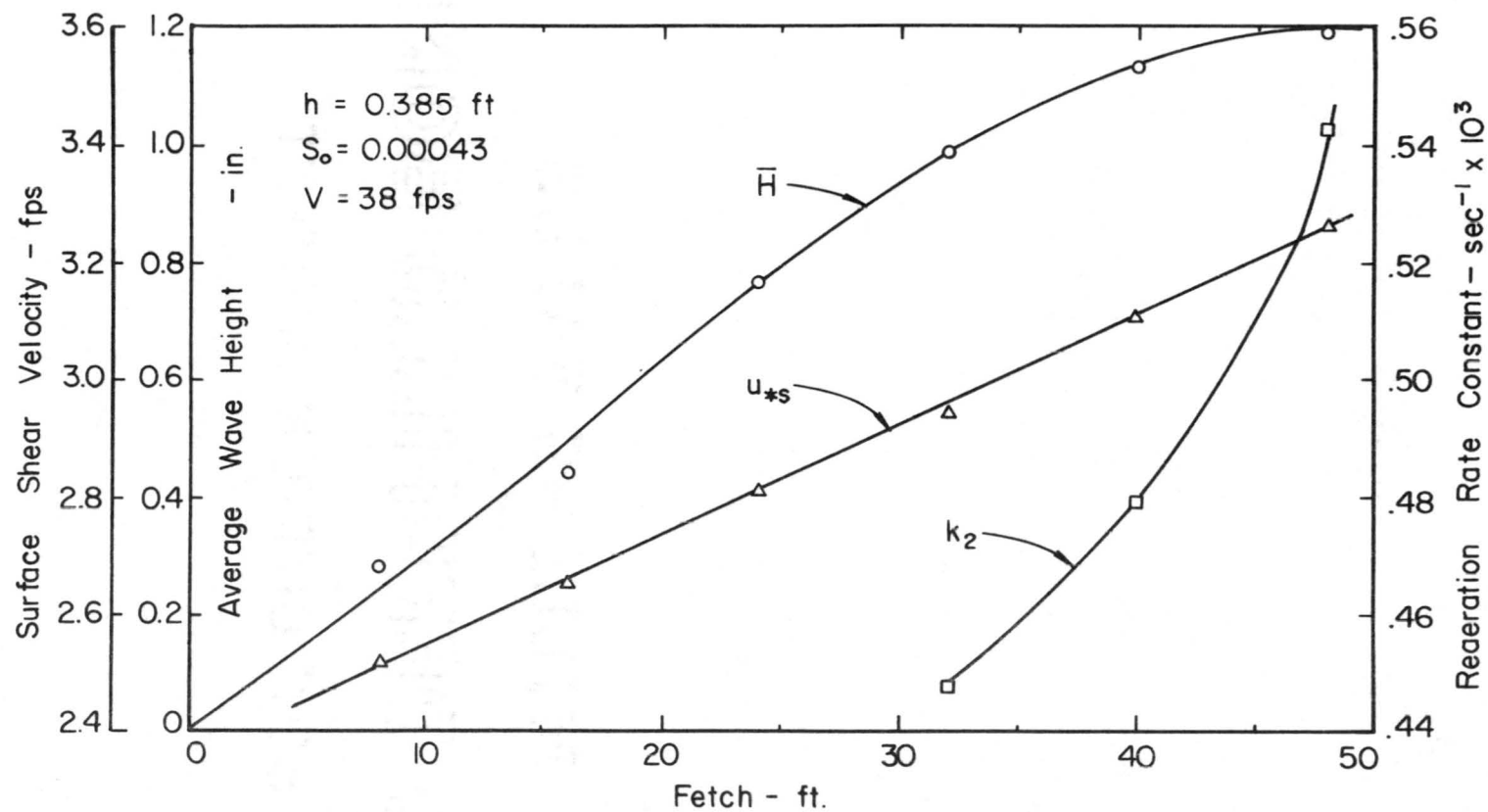


Fig. 26 - Variation of the Surface Shear Velocity, Average Wave Height and the Reaeration Coefficient with Fetch.

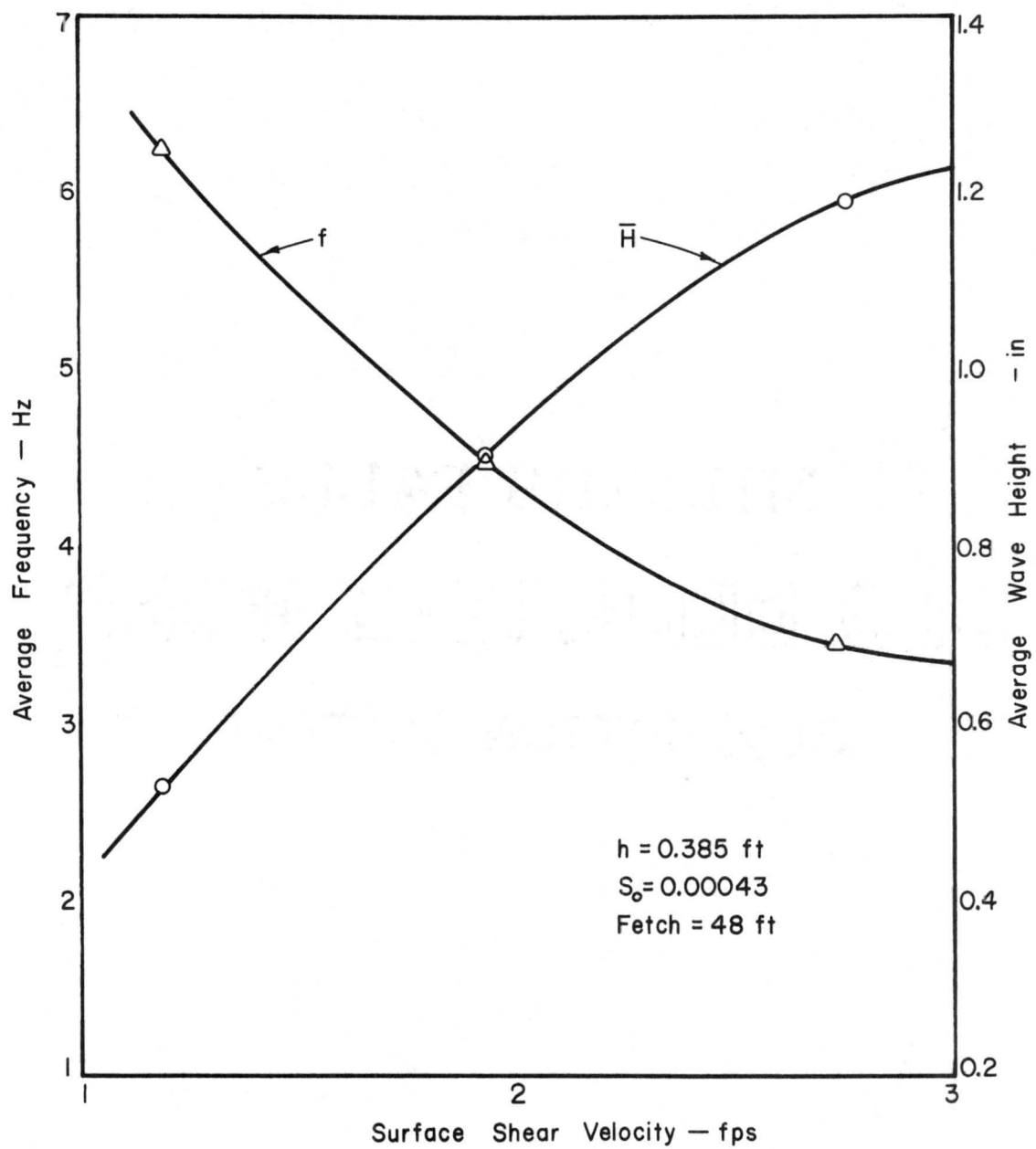


Figure 27 — Variations of \bar{H} and f with u_{*s} at a Fixed Position in the Flume

effects of viscosity or turbulent shear stresses, as reflected in the nonuniform velocity distributions, are disregarded by the equation.

An investigation of wave speed deviation from classical theory for gravity waves in moving water was made by Francis and Dudgeon (1967), who made an attempt to determine a relationship between measured wave phase velocity and the theoretical wave velocity based on wave length, calculated from Equation (75). The graph of c_t vs $\bar{c}_e + U$, taken from their paper is shown in Figure 28a. A plot similar to that of Francis and Dudgeon, was prepared from the data and is shown in Figure 28b. The theoretical wave speed was calculated from Equation (75) using the measured wave length, and was plotted against the difference $\bar{c}_e - U$. In all cases, the measured phase speed of significant waves were larger than the theoretical values, c_t . This deviation could be attributed to the increase in wave velocity associated with surface drift, and to the fact that the waves are finite in amplitude.

In a recent thesis, Trawle (1969) discusses results of an experimental study of wave speed deviation from classical theory for gravity waves in moving water. Trawle presented an empirical analysis in an attempt to develop a correction factor for wind wave phase velocity which could be applied to the theoretical phase velocity. He postulated an additive model of the form

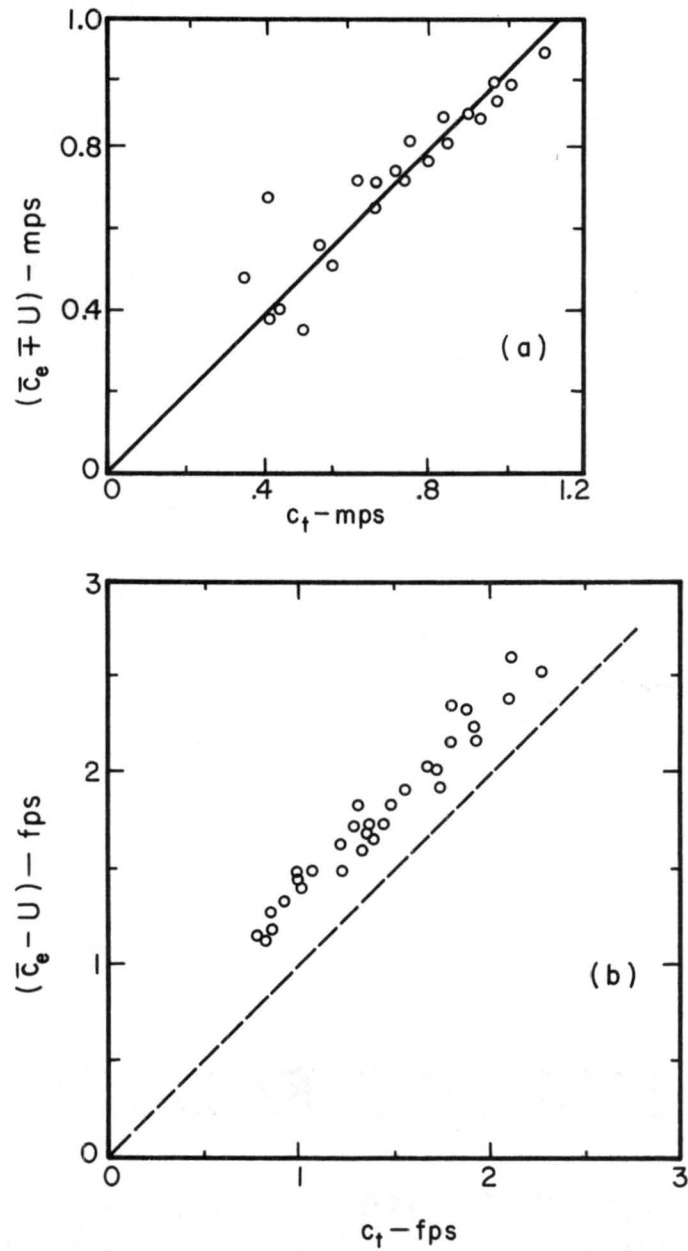


Figure 28 - Observed Wave Speed, Relative to a Fixed Point,
 Compared with Theoretical Small Amplitude Waves.
 (a) Francis and Dudgeon, (b) This investigation

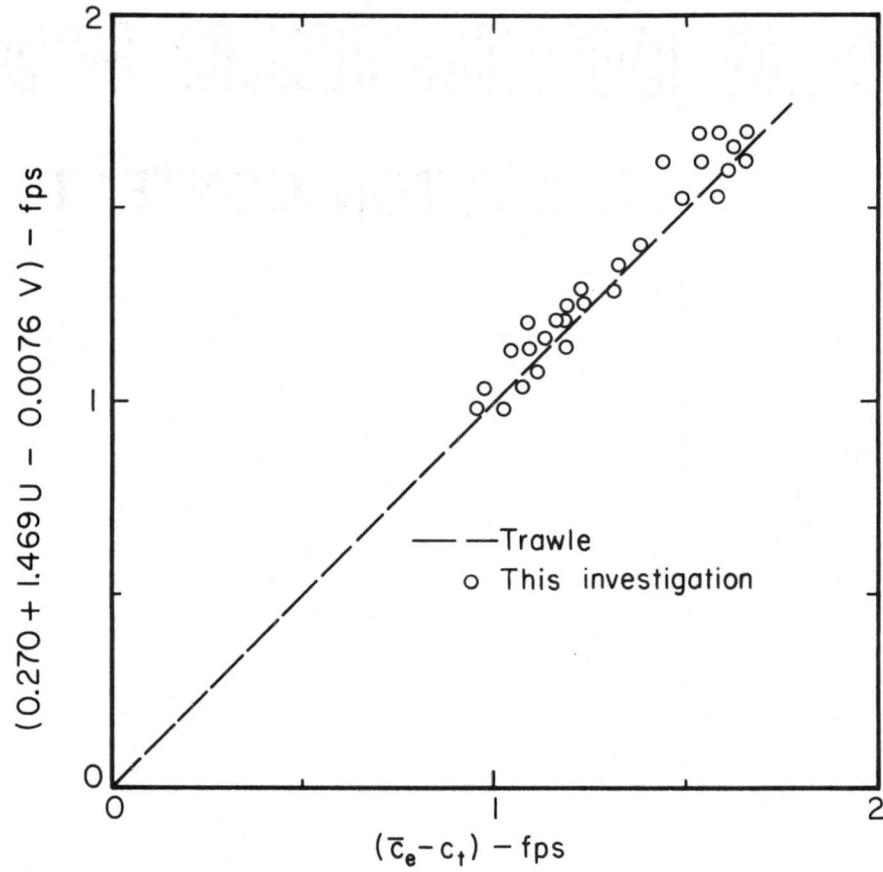


Figure 29—Comparing the Results of this Investigation to those Reported by Trawle

$$\bar{c}_e - c_t = a_1 + a_2 U + a_3 V$$

where a_1 , a_2 , and a_3 are constant. For concurrent flow, his analysis yielded the following empirical equation

$$\bar{c}_e - c_t = 0.270 + 1.469 U - .0076 V \quad (76)$$

Using the data of this investigation, a plot of $(\bar{c}_e - c_t)$ versus $(0.270 + 1.469 U - .0076 V)$ is shown in Figure 29. The small deviations of the data from the 1:1 correspondence, indicates a good agreement between our results and those reported by Trawle.

Roughness Effect on Reaeration Rates

Experimental results clearly indicate that reaeration rates are significantly increased when waves appear on the surface. Figure 26 shows the increase of k_2 with fetch, for a given wind velocity. The variation of k_2 with \bar{H} is illustrated in Figure 30. The increase is often very much more than can be accounted for by the increase in surface area. An increase of surface area due to the waves action has been estimated, by the author, by assuming a sinusoidal waves with $\bar{\lambda} = 10 \bar{H}$. The resultant surface - area increase was about 15 percent. This amount of increase was not enough to account for the total increase of reaeration by the wavy surface. The total increase in

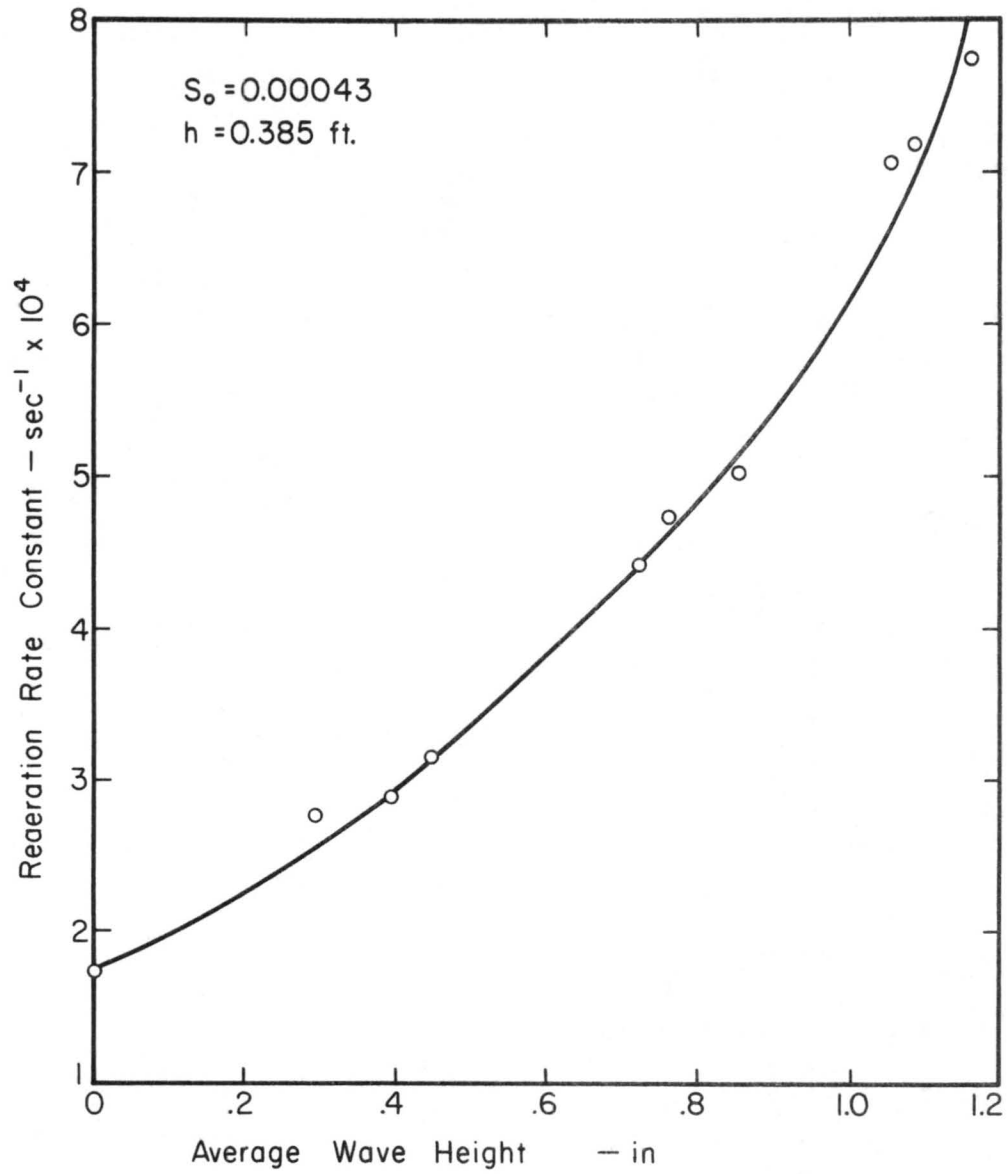


Figure 30 - Variation of Reaeration Rate with the Average Wave Height

rates of reaeration ranged from 55 percent to 175 percent, depending on the wind speed. Thus, the increase is to be sought, rather, in the dynamic effect of waves on the reaeration rates.

Dynamic effect of waves on reaeration - As waves grow by wind action from ripples to the well-developed gravity waves, the effect on reaeration and momentum transfer may be considered in terms of an increasingly rough surface. The process of interaction between water waves and the turbulent shearing flow overhead is a highly nonlinear one which appears to be basically equivalent to the interaction of flow with a rough solid surface. Because separation of flow near solid roughness elements is known to be responsible for modification of flow, it is concluded that similar behavior is true for air-water wave interaction.

Schooley's (1963) and P. Chang's (1968) flow visualization experiments do suggest the presence of a separation region and there are some physical grounds for expecting this effect. In general, flow separation is found when slowly moving air near the surface moves into a region of adverse pressure gradient.

Many features observed in the air flow near the waves can now be explained in the light of flow separation. The lower portion of the air velocity profile deviates from the logarithmic profile. In the presence of separation,

the air, as it creeps forward from over a crest to a trough, will be decelerated and turned back by the action of adverse pressure gradient, moves down and returns toward the crest. This orbital motion of the air in the separation region results in a relatively large magnitude of the vertical turbulent component near the surface. In other words, the eddy diffusivity for momentum and mass, being proportional to the turbulent velocity fluctuation, is larger with separation near the waves, with a corresponding augmentation of reaeration rate.

Since the turbulent diffusion coefficient, at the surface, was given as a function of the surface shear velocity, u_{*s} , the increase in reaeration, due to the dynamic effect of waves, is embedded in the term u_{*s} .

Chapter VII

SUMMARY AND CONCLUSIONS

Summary

The investigation presented herein had three major objectives: (1) to explain the transfer mechanism of oxygen from the moving air to flowing streams and rivers; (2) to develop a method for estimating oxygen absorption rates in streams and rivers, with wind blowing; and (3) to test some of the models used by predicting the reaeration coefficient, with no wind blowing over the water surface.

Before starting the experimental investigation for this problem a review of literature was a necessary step to give a basis for the current investigation. An examination of the theories of the gas absorption process has been presented, and some of the ideas proposed were adopted in the theoretical development of this work.

The different theories agreed with the basic oxygen - sag equation:

$$\frac{dD}{dt} = - K_2 D \quad (5)$$

The differences were, however, in the definition of K_2 . The most reasonable definition of K_2 was advanced by Krenkel (1960), who formulated the following expression for K_2

$$k_2 \propto \frac{D_T}{v} r \quad (18)$$

This expression was adopted in the theoretical development of this work, resulting in the equation for predicting k_2 in natural streams and rivers with wind blowing over the water surface:

$$k_2 = c R_{sh} \frac{u_{*c}}{h} \quad (67)$$

where $R_{sh} = \frac{u_{*s} h}{v}$. The development of Equation (67), with the assumptions used, was tested against the experimental data of this study.

Conclusions

The results of the study point to several conclusions which may be drawn and some aspects which need further research.

Reaeration with no wind - The analysis of the data yielded the following predictive equations.

$$k_2 = 3.182 \frac{U}{R^{3/2}} \quad (69)$$

$$k_2 = 0.000053 \frac{D_L}{R^2} \quad (70)$$

$$k_2 = 0.000776 \frac{u_{*b}}{R} \quad (71)$$

These results indicated that the data obtained from this investigation are in good agreement with those reported by Isaacs-Gaudy, Equation (46), and by Krenkel, Equation (42). However, the values of this investigation were about 20 percent lower than those of the natural stream data of Churchill, Equation (47), and larger than those reported by Thackston, Equation (38), by a factor of about 3.6. The discrepancy between the results and those of Churchill was attributed to channel geometry. But, no explanation for the apparent differences between the results of this investigation and of Thackston could be found. It was only possible to conclude that more laboratory investigations are needed, which might resolve the discrepancy.

Reaeration with wind - The experimental data were analyzed using a multiple regression analysis, and it was concluded that k_2 was related to R_{sh} and u_{*c} as follows:

$$k_2 = (2.66 \times 10^{-8}) R_{sh}^{1.0414} \frac{u_{*c}^{1.0583}}{h} \quad (73)$$

for which the multiple correlation coefficient was 0.9943.

The rather high degree of correlation between the variables and the fact that the constants 1.0414 and 1.0583 are close to their theoretical values of 1.0, gave support to the theoretically based form of the relationship

$$k_2 = C R_{sh} \left(\frac{u_{*c}}{h} \right) \quad (67)$$

A second analysis of the data was performed, using Equation (67). The analysis yielded the predictive equation

$$k_2 = (3.13 \times 10^{-8}) R_{sh} \frac{u_{*c}}{h} \quad (74)$$

in which the correlation coefficient was 0.989.

The advantages and the limitations of the developed equation were outlined in the text of this dissertation.

Equation (74) constitutes the main contribution of this investigation, and represents a significant step toward including the fundamentals of the oxygen transfer mechanism from the wind to flowing streams and rivers in oxygen calculations. However, the development of this equation does not imply that the problem of reaeration prediction with wind is solved. It is the belief that further work is needed, either to improve the formula, or until the phenomenon of gas transfer with wind is completely understood.

Properties of the water surface - The experimental results demonstrated that on a qualitative basis, the rates of growth of the wind generated waves are compatible with the theoretical proposals of Phillips and Miles which predict an initial linear rate of growth followed by an exponential increase.

All wave data have been presented and analyzed, and the results are in good agreement with those reported by previous investigators.

The effect of surface roughness on reaeration - It was concluded that the reaeration rates are significantly increased when waves appear on the surface. The increase is often very much more than can be accounted for by the increase in surface area. Thus, a dynamic effect of separation, at the lee side of wave, was concluded to be the major factor influencing reaeration rates.

It was not intuitively obvious how separation could influence reaeration. One could argue, however, that separation could be associated with a relatively large magnitude of the vertical turbulent component near the surface. In other words, the eddy diffusivity for momentum and mass is larger with separation near the waves, with corresponding augmentation of reaeration rate.

Although the phenomenon of separation has been used in many places as a basis of physical explanation, it is not clear whether or not flow separation of wind over

water waves is a general occurrence. Thus, it is the author's belief that the concept of separation at the lee side of wave needs further investigation.

BIBLIOGRAPHY

BIBLIOGRAPHY

- Adney, W.E. and Becker, H.G., (1919); "The Determination of the Rate of solution of Atmospheric Nitrogen and Oxygen by Water," Philosophical Magazine, Vol. 38, pp. 317-337.
- Al-Saffar, A.M., (1964); "Eddy Diffusion and Mass Transfer in Open Channel Flow," Ph.D Dissertation, Civil Engineering Department, University of California, Berkeley, California, 138 p.
- Benjamin, T.B., (1959); "Shearing Flow over a Wavy Boundary," J. of Fluid Mech., Vol. 6, pp. 161-205.
- Chang, Po-cheng, (1968); "Laboratory Measurements of Air Flow over Wind Waves Following the Water Surface," Ph.D Dissertation, Department of Civil Engineering, Colorado State University, Fort Collins, Colorado, 126 p.
- Churchill, M.A., (1960); "Solubility of Atmospheric Oxygen in Water," J. of the Sanitary Engineering Division, American Society of Civil Engineering, Vol. 86, No. SA4, pp. 41-53.
- Churchill, M.A., Elmore, H.L. and Buckingham, R.A., (1962); "Prediction of Steam Reaeration Rates," J. of the Sanitary Engineering Division, American Society of Civil Engineering, Vol. 88, No. SA4, pp. 1-46.
- Danckwerts, P.V., (1951); "Significance of Liquid Film Coefficients in Gas Absorption," Industrial and Engineering Chemistry, Vol. 43, No. 6, pp. 1460-1467.
- Diachishin, A.N., (1958); Discussion of "Mechanism of Reaeration in Natural Streams," by D.J. O'Connor, Transactions, Am. Soc. of Civil Eng., Vol. 123, pp. 672-677.
- Dobbins, W.E., (1956); "The Nature of the Oxygen Transfer Coefficient in Aeration Systems," Part 2-1 of Biological Treatment of Sewage and Industrial Wastes, by McCabbe and Eckenfelder, Reinholt, New York, pp. 141-148.
- Dobbins, W.E., (1962); "Mechanism of Gas Absorption by Turbulent Liquids," presented at International Conference on Water Pollution Research, London, England, pp. 61-69.

- Kalinske, A.A. and Pien, C.L., (1944); "Eddy Diffusion," Industrial and Engineering Chemistry, Vol. 36, pp. 220-223.
- Keulegan, G.H., (1951); "Wind Tides on Small Closed Channels," J. Res. Nat. Bureau of Standards, Vol. 46, No. 5, pp. 358-381.
- Kinsman, B., (1965); Wind Waves (Their Generation and Propagation on the Ocean Surface), Prentice-Hall, Inc., Englewood Cliffs, N.J., 676 p.
- Kishinevski, M., (1955); "Two Approaches to the Theoretical Aspects of Gas Absorption," J. of Appl. Chem., USSR, Vol. 28, pp. 881-886.
- Kishinevski, M. and Serebryanski, V.T., (1955); "The Mechanism of Mass Transfer at the Gas-Liquid Interface with Vigorous Stirring," J. of Appl. Chem., USSR, Vol. 29, pp. 29-33.
- Krenkel, P.A., (1960); "Turbulent Diffusion and the Kinetics of Oxygen Absorption," Ph.D Dissertation, University of California, Berkeley, California, 142 p.
- Krenkel, P.A. and Orlob, G.T., (1963); "Turbulent Diffusion and the Reaeration Coefficient," Transactions, Am. Soc. of Civil Eng., Vol. 128, No. 3491, pp. 293-323.
- Lamb, Sir H., (1932); Hydrodynamics, Cambridge Press, 738 p.
- Levich, V.G., (1962); Physicochemical Hydrodynamics, Englewood Cliffs, N.J., Prentice-Hall, Inc., 700 p.
- Longuet-Higgins, M.S., (1962); "The Directional Spectrum of Ocean Waves and Processes of Wave Generation," Proc. Roy. Soc. London, A, Vol. 265, pp. 286-315.
- Masch, F.D., (1963); "Mixing and Dispersion of Wastes by Wind and Wave Action," Int. J. of Air Wat. Poll., Vol. 7, pp. 697-720.
- Miles, J.W., (1957); "On the Generation of Surface Waves by Shear Flows," J. of Fluid Mech., Vol. 3, pp. 185-204.
- Miles, J.W., (1959); "On the Generation of Surface Waves by Shear Flows, Part 2," J. of Fluid Mech., Vol. 6, pp. 568-582.
- Monin, A.S., (1959); "General Survey of Atmospheric Diffusion," Advances in Geophysics, Vol. 6, Academic Press, pp. 29-40.

- Munk, W.H., (1955); "Wind Stress on Water: an hypothesis," Quarterly J., Roy. Met. Soc., Vol. 81, pp. 320-332.
- O'Connor, D.J. and Dobbins, W.E., (1958); "Mechanism of Reaeration in Natural Streams," Transactions, Am. Soc. of Civil Eng., Vol. 123, No. 2934, pp. 641-666.
- Owens, M., Edwards, R.W. and Gibbs, J.W., (1964); "Some Reaeration Studies in Streams," Int. J. of Air Water Poll., Vol. 8, pp. 469-486.
- Pearson, E.A., (1958); Discussion of paper given by D.J. O'Connor, Technical Report W58-2, Seminar on Oxygen Relationships in Streams, Taft Sanitary Engineering Center.
- Phillips, O.M., (1957); "On the Generation of Waves by Turbulent Wind," J. of Fluid Mech., Vol. 2, pp. 417-445.
- Plate, E.J., (1969); "Water Surface Velocities Induced by Wind Shear," Unpublished Paper, Department of Civil Engineering, Colorado State University, Fort Collins, Colorado.
- Plate, E.J. and Goodwin, C.R., (1965); "The Influence of Wind on Open Channel Flow," Paper presented at the Special Conf. on Coastal Eng., Am. Soc. of Civil Eng., Santa Barbara, California, pp. 391-423.
- Plate, E.J. and Hidy, G.M., (1967); "Laboratory Study of Air Flowing over a Smooth Surface onto Small Water Waves," J. Geophys. Res., Vol. 72, pp. 4644.
- Sayre, W.W., (1968); "Dispersion of Mass in Open-Channel Flow," Hydraulic Paper No. 3, Colorado State University, Fort Collins, Colorado, 73 p.
- Sayre, W.W. and Chang, F.M., (1966); "A Laboratory Investigation of Open Channel Dispersion Process for Dissolved, Suspended and Floating Dispersants," Open File Report, U.S. Geol. Survey, Water Resources Div., Fort Collins, Colorado, 210 p.
- Schlichting, H., (1965); Boundary Layer Theory, McGraw-Hill Company, New York.
- Schooley, A.H., (1963); "Simple Tools for Measuring Wind Fields above Wind-Generated Water Waves," J. of Geophys. Res., Vol. 68, pp. 5497-5504.

- Stirba, C. and Hurt, D.M., (1955); "Turbulence in Falling Liquid Films," J. Am. Inst. of Chem. Eng., Vol. 1, No. 2, pp. 178-182.
- Streeter, H.W., (1935); "The Reaeration Factor and Oxygen Balance," Sewage Works Journal, May, p. 534.
- Streeter, H.W. and Phelps, E.B., (1925); "A Study of the Pollution and Natural Purification of the Ohio River, III," Public Health Bulletin No. 146, Washington, 16 p.
- Taylor, G.I., (1954); "The Dispersion of Matter in Turbulent Flow through a Pipe," Proc. Roy. Soc. London, A, Vol. 223, pp. 446-488.
- Thackston, E.L., (1966); "Longitudinal Mixing and Reaeration in Natural Streams," Ph.D Dissertation, Vanderbilt University, 212 p.
- Thackston, E.L. and Krenkel, P.A., (1964); Discussion of "BOD and Oxygen Relationships in Streams," by W.E. Dobbins, J. of the Sanitary Engineering Division, Am. Soc. of Civil Eng., Vol. 90, No. SA3, pp. 53-78.
- Trawle, M.J., (1968); "Wind Waves on Open Channel Flow," M.S. Thesis, Department of Civil Engineering, Colorado State University, Fort Collins, Colorado, 81 p.
- Truesdale, G.A. and Van Dyke, (1958); "The Effect of Temperature on the Aeration of Flowing Water," Water and Waste Treatment J., Vol. 7, No. 9, May-June.
- Ursel, F., (1956); "Wave Generation by Wind," Survey in Mechanics (ed. G.K. Batchelor and R.W. Davies), Cambridge University Press, Cambridge, pp. 216-249.
- Vanoni, V.A., (1946); "Transportation of Suspended Sediment by Water," Transactions, Am. Soc. of Civil Eng., Vol. III, pp. 67-133.
- Vanoni, V.A. and Brooks, N.H., (1957); "Laboratory Studies of the Roughness and Suspended Load of Alluvial Streams," Report M.R.D. No. 11, Sedimentation Laboratory, Cal. Inst. of Tech., Pasadena, California, pp. 100-106.
- Whitman, W.G., (1923); "Two-film Theory of Gas Absorption," Chem. and Metallurgical Engineering, Vol. 29, p. 146.
- Whitman, W.G. and Lewis, W.K., (1924); "Principles of Gas Absorption," Industrial and Engineering Chemistry, Vol. 16, pp. 1215-1220.

APPENDIX

TABLE 1 - SUMMARY OF LABORATORY DATA

Series 1 : Reaeration with no wind

S_o	h		U	k_2	T
ft/ft	ft	in	fps	sec ⁻¹	°C
$\times 10^3$				$\times 10^4$	
1.000	.158	1.90	.656	3.85	21.7
	.254	3.05	.770	3.63	20.8
	.328	3.94	1.000	2.89	22.6
	.385	4.62 ←	1.021	2.93	21.1
	.418	5.01	1.068	2.50	22.6
	.477	5.72	1.100	2.67	23.2
0.430	.185	2.24	.546	2.52	21.9
	.254	3.05	.649	2.45	23.0
	.337	4.04	.713	2.04	23.2
	.385	4.62 ← →	.735	1.67	23.2
	.419	5.03	.775	1.93	22.6
	.468	5.61	.904	1.88	23.9

TABLE 2 - SUMMARY OF LABORATORY DATA

Series 2 : Reaeration with Wind

$$h = 0.385 \text{ ft.}$$

S_o	Test Section	V	U	$\frac{dp}{dx}$	k_2	T
ft/ft		fps	fps	lb/ft ³	sec ⁻¹	°C
$\times 10^3$				$\times 10^4$	$\times 10^4$	
1.000	1 - 4	22	1.039	- 4.52	3.89	21.0
	1 - 4	30	1.089	- 8.17	6.43	20.7
	1 - 4	38	1.196	-14.87	8.89	20.6
	1 - 3	22	1.039	- 4.48	3.84	21.8
	1 - 3	30	1.089	- 7.88	6.31	21.7
	1 - 3	38	1.196	-14.45	8.05	21.5
	1 - 2	22	1.039	- 4.63	3.81	21.6
	1 - 2	30	1.089	- 7.41	6.18	21.8
	1 - 2	38	1.196	-13.75	7.50	21.9
0.430	1 - 4	22	0.765	- 4.41	2.72	21.2
	1 - 4	30	0.833	- 8.31	3.98	20.7
	1 - 4	38	0.987	-14.69	5.32	20.7
	1 - 3	22	0.765	- 4.27	2.64	21.8
	1 - 3	30	0.833	- 8.18	3.74	21.6
	1 - 3	38	0.987	-14.41	4.79	21.5
	1 - 2	22	0.765	- 3.92	2.59	21.5
	1 - 2	30	0.833	- 7.80	3.55	21.8
	1 - 2	38	0.987	-14.05	4.48	21.8

TABLE 3 - WAVES DATA

h = 0.385 ft.

S_o	V	U	Fetch	\bar{H}	$\bar{\lambda}$	f	c_e	c_t
ft/ft	fps	fps	ft	in.	in.	cps	fps	fps
$\times 10^{+3}$								
1.000	22	1.039	8	0.04	1.61	16.13	2.17	0.83
	30	1.083	8	0.05	2.38	12.82	2.54	1.01
	38	1.196	8	0.14	3.64	9.27	2.82	1.24
	22	1.039	16	0.07	1.81	14.92	2.25	0.88
	30	1.083	16	0.10	3.61	9.05	2.72	1.24
	38	1.196	16	0.26	4.42	7.91	2.91	1.39
	22	1.039	24	0.11	2.07	13.70	2.37	0.94
	30	1.083	24	0.14	4.21	8.30	2.91	1.34
	38	1.196	24	0.34	5.95	6.27	3.11	1.59
	22	1.039	32	0.23	2.80	10.81	2.53	1.10
	30	1.083	32	0.27	5.56	6.47	3.00	1.54
	38	1.196	32	0.44	6.82	5.64	3.21	1.71
	22	1.039	40	0.31	3.70	8.33	2.57	1.26
	30	1.083	40	0.36	6.69	5.54	3.09	1.73
	38	1.196	40	0.49	8.83	4.64	3.42	1.95
	22	1.039	48	0.42	4.47	7.27	2.71	1.38
	30	1.083	48	0.49	7.85	5.26	3.44	1.83
	38	1.196	48	0.55	10.67	4.26	3.79	2.13
0.430	22	0.765	8	0.05	1.55	14.92	1.93	0.81
	30	0.833	8	0.20	2.56	10.80	2.30	1.05
	38	0.987	8	0.28	4.02	7.30	2.69	1.31
	22	0.765	16	0.10	1.82	13.25	2.02	0.88
	30	0.833	16	0.28	4.00	7.32	2.44	1.31
	38	0.987	16	0.43	5.35	6.32	2.82	1.51
	22	0.765	24	0.20	2.59	10.00	2.16	1.05
	30	0.833	24	0.39	5.05	6.08	2.56	1.47
	38	0.987	24	0.76	7.24	4.83	2.91	1.76
	22	0.765	32	0.27	3.61	7.52	2.27	1.24
	30	0.833	32	0.62	6.09	5.44	2.76	1.61
	38	0.987	32	0.99	8.99	4.18	3.13	1.96
	22	0.765	40	0.32	4.26	6.67	2.38	1.35
	30	0.833	40	0.82	7.71	4.63	2.98	1.81
	38	0.987	40	1.13	10.61	3.80	3.36	2.13
	22	0.765	48	0.53	4.65	6.25	2.42	1.41
	30	0.833	48	0.90	8.49	4.46	3.16	1.91
	38	0.987	48	1.19	12.22	3.44	3.50	2.29

TABLE 4 - SUMMARY OF DATA

Series 2: Reaeration with Wind

$$h = 0.385$$

S_o ft/ft $\times 10^3$	Section	S_c ft/ft $\times 10^3$	V_1 fps	\bar{H} in.	$\bar{\lambda}$ in.	f cps	\bar{c}_e fps	k_2 sec^{-1} $\times 10^4$	u_{*c} fps	u_{*s} fps	R_{sh} $\times 10^{-4}$
1.000	3-4	1.074	24.24	0.37	4.09	7.80	2.64	4.12	0.115	1.22	4.593
	3-4	1.128	32.95	0.43	7.27	5.40	3.27	6.94	0.118	1.93	7.280
	3-4	1.183	42.31	0.52	9.75	4.45	3.61	12.10	0.121	2.82	10.638
	2-3	1.074	23.90	0.27	3.25	9.57	2.55	3.97	0.115	1.19	4.497
	2-3	1.101	32.34	0.32	6.13	6.01	3.05	6.80	0.117	1.88	7.080
	2-3	1.176	41.50	0.47	7.33	5.14	3.32	10.98	0.120	2.73	10.295
	2-4	1.074	24.00	0.33	3.64	9.04	2.62	4.05	0.115	1.20	4.528
	2-4	1.106	32.54	0.38	6.71	5.87	3.22	6.81	0.117	1.89	7.146
	2-4	1.179	41.63	0.50	8.75	4.95	3.50	11.32	0.121	2.74	10.341
0.430	3-4	0.500	24.16	0.43	4.46	6.46	2.40	3.10	0.079	1.21	4.574
	3-4	0.562	32.96	0.86	8.10	4.55	3.07	5.02	0.084	1.93	7.285
	3-4	0.663	41.57	1.16	11.42	3.62	3.43	7.75	0.091	2.73	10.318
	2-3	0.496	23.87	0.30	3.94	7.20	2.33	2.79	0.078	1.19	4.489
	2-3	0.558	32.39	0.72	6.90	5.09	2.87	4.43	0.083	1.88	7.107
	2-3	0.658	41.44	1.06	9.80	3.99	3.25	7.06	0.090	2.72	10.272
	2-4	0.498	23.92	0.40	4.13	6.94	2.35	2.90	0.079	1.19	4.505
	2-4	0.559	32.59	0.76	7.29	4.95	2.91	4.73	0.083	1.93	7.277
	2-4	0.660	41.50	1.09	10.61	3.81	3.32	7.17	0.090	2.73	10.291